

# Endless self-avoiding walks

Nathan Clisby

ARC Centre of Excellence for Mathematics and Statistics of Complex Systems,  
Department of Mathematics and Statistics,  
The University of Melbourne, VIC 3010, Australia

March 13, 2013

## Abstract

We introduce a self-avoiding walk model for which end-effects are completely eliminated. We enumerate the number of these walks for various lattices in dimensions two and three, and use these enumerations to study the properties of this model. We find that endless self-avoiding walks have the same connective constant as self-avoiding walks, and the same Flory exponent  $\nu$ . However, there is no power law correction to the exponential number growth for this new model, i.e. the critical exponent  $\gamma = 1$  exactly in any dimension. In addition, the number growth has no analytic corrections to scaling, and we have convincing numerical evidence to support the conjecture that the amplitude for the number growth is a universal quantity. The technique by which end-effects are eliminated may be generalized to other models of polymers such as interacting self-avoiding walks.

**Keywords** self-avoiding walk; critical exponent; enumeration; critical amplitude

## 1 Introduction

Self-avoiding walks (SAW) on a regular lattice are an important model in statistical mechanics with a long history [1]. An  $n$ -step SAW is a map  $\omega$  from the integers  $\{0, 1, \dots, n\}$  to sites on the lattice, with  $\omega(0)$  conventionally at the origin, and  $|\omega(i+1) - \omega(i)| = 1$ , and  $\omega(i) \neq \omega(j) \forall i \neq j$ . The SAW model is the  $N \rightarrow 0$  limit of the  $N$ -vector model, which includes the Ising model as the  $N = 1$  case, and as such it is an important model for the theoretical understanding of critical phenomena [2]. Self-avoiding walks are in the same universality class as polymers in a good solvent, and thus the model also has an important physical interpretation. Much is known about self-avoiding walks, particularly in dimensions  $d \geq 4$  [3, 4], and considerable progress has been made in understanding self-avoiding walks in two dimensions [5, 6, 7], but an exact solution remains elusive for any dimension bar the trivial case  $d = 1$ .

The most important quantities which characterize SAW are the number of SAW of length  $n$ ,  $c_n$ , and measures of the size of the walk, such as the square end-to-end distance,  $r_n$ . In the following definitions we assume that summations are performed over the set of self-avoiding walks of length  $n$ :

$$c_n = \sum_{|\omega|=n} 1 \quad (1.1)$$

$$r_n = \sum_{|\omega|=n} |\omega(n)|^2 \quad (1.2)$$

We abuse notation by allowing  $|\omega|$  to measure the number of steps of a walk  $\omega$ , while  $|\omega(n)|^2$  is the square of the Euclidean norm of the site  $\omega(n)$ .

The asymptotic behavior of  $c_n$  and  $r_n$  is characterized by certain quantities of fundamental interest, namely the connective constant,  $\mu$ , which is lattice dependent, and the critical exponents  $\gamma$  and  $\nu$  which are universal. We have

$$c_n \sim A\mu^n n^{\gamma-1} \left( 1 + \frac{a_1^*}{n} + \frac{a_2^*}{n^2} + \dots + \frac{b_0^*}{n^{\Delta_1}} + \dots \right) + \text{AF}, \quad (1.3)$$

$$r_n \sim AD\mu^n n^{2\nu+\gamma-1} \left( 1 + \frac{f_1^*}{n} + \frac{f_2^*}{n^2} + \dots + \frac{g_0^*}{n^{\Delta_1}} + \dots \right) + \text{AF}, \quad (1.4)$$

$$\rho_n \sim Dn^{2\nu} \left( 1 + \frac{l_1^*}{n} + \frac{l_2^*}{n^2} + \dots + \frac{m_0^*}{n^{\Delta_1}} + \dots \right) + \text{AF}, \quad (1.5)$$

where we define the mean square end-to-end distance as  $\rho_n \equiv r_n/c_n$ . The corrections in (1.3)–(1.5) with integer powers of  $n$  are the analytic corrections to scaling, while  $\Delta_1$  is the exponent of the leading non-analytic correction to scaling. There are additional higher order analytic corrections with exponents  $-3, -4, \dots$ , and non-analytic corrections with exponents  $\Delta_2, \Delta_3, \dots$ . The higher order corrections to scaling involve arbitrary mixed terms as well, of the general form  $\text{const.}/n^{j_0+j_1\Delta_1+j_2\Delta_2+j_3\Delta_3+\dots}$ , with non-negative integers  $j_i$ . In (1.3)–(1.5), AF denotes the possible contribution of the so-called anti-ferromagnetic term which occurs for bipartite lattices such as the square lattice and the simple cubic lattice. This term alternates in sign, and is sub-leading as the exponent arises from polygon-like configurations.

See [8] for extensive discussions and analysis of the correct asymptotic form for two-dimensional SAW, and [9] for a discussion of the full asymptotic form for three-dimensional SAW.

Due to the importance of SAW, in the absence of an exact solution it is desirable to find simpler models. Recent progress has been made in finding interesting solvable models of walks, with non-trivial critical exponents, such as prudent walks [10, 11]. Another recent paper [12, 13] takes a different approach, developing a prescription to discretize SLE, resulting in a self-avoiding walk which is a finite piece of an infinite SLE curve.

Other models which are related to SAW are self-avoiding returns and polygons (SAR and SAP respectively) and bridges. A self-avoiding return (SAR) is a SAW which is forced to return to the origin, i.e. an  $n$ -step SAR is identified with an  $n - 1$ -step SAW with  $|\omega(n - 1) - \omega(0)| = 1$ . An SAP is an *unrooted unoriented* SAR, and so there are exactly  $2n$  corresponding SAR for each  $n$ -step SAP. Bridges are a subset of SAW with an additional condition on the  $x$ -coordinates of a walk:  $\omega_1(0) < \omega_1(i) \leq \omega_1(n)$  with  $0 < i \leq n$ . Both SAP and bridges have the same connective constant as SAW, and the same size exponent  $\nu$  as SAW, but different critical exponents for their growth in number.

In this paper we introduce a new variant of SAW, which we call endless self-avoiding walks, or eSAW. We will prove that this new model has the same connective constant  $\mu$  as SAW, and argue that it has the same critical exponent  $\nu$  as SAW but with number growth exponent  $\gamma_e = 1$  in any dimension. The number growth has no analytic corrections to scaling, and we find strong numerical evidence that the amplitude  $A_e$  of the number growth is a universal quantity.

We will study eSAW on various two-dimensional and three-dimensional lattices, in particular the square, honeycomb, triangular, union jack, simple cubic, body centered cubic (bcc), and face centered cubic (fcc) lattices. The model can be naturally extended to other lattices, and also to other models of walks as described in Sec. 5.

## 1.1 Outline

We will first introduce the endless self-avoiding walk model in Sec. 2, and discuss its expected properties. We will then describe the enumeration method in Sec. 3, and analyze the resulting enumerations to estimate critical parameters for eSAW in Sec. 4. In Sec. 5 we will discuss various aspects of the eSAW model, and finally conclude in Sec. 6.

## 2 Endless self-avoiding walks

The basic idea for constructing the model is extremely simple: we start with the set of self-avoiding walks, and endless self-avoiding walks are the subset of walks which are still self-avoiding after they have been concatenated with copies of themselves head-to-tail *ad infinitum*. An example of an eSAW on the square lattice is shown on the left in Fig. 2.1, with the root point shown as a solid circle and the concatenated copies as dotted lines, while on the right is a SAW which is not an eSAW. Because the walk is extended to infinity, sites on the walk are indistinguishable and end-effects are completely eliminated. This definition of eSAW is applicable for any lattice.



Figure 2.1: An example eSAW,  $\omega_{\text{ex}}$ , on the left; on the right is a SAW which is not an eSAW.

An alternative, illuminating definition of eSAW may be given in terms of words, where we define the walk in terms of sequences of steps rather than sites on a lattice. We now specialize to  $\mathbb{Z}^d$  for the sake of concreteness, but the argument is similar for other lattices. Let us denote the steps in the positive axis directions as  $1, 2, \dots, d$ , and the steps in the negative axis directions as  $\bar{1}, \bar{2}, \dots, \bar{d}$ . Then SAW of  $n$  steps correspond to the set of words

which contain no loops, i.e. for which there are no sub-words with equal numbers of 1 and  $\bar{1}$ , 2 and  $\bar{2}$ ,  $\dots$ ,  $d$  and  $\bar{d}$ . Given a walk, the infinite word which results from concatenating that word with itself indefinitely is an endless walk. If the infinite word has no loops, then the walk is an endless SAW in correspondence with our earlier definition. E.g., if we consider the example SAW from Fig. 2.1,  $\omega_{\text{ex}} = 12121\bar{2}$ , then the corresponding infinite word is  $\dots 12121\bar{2}12121\bar{2}12121\bar{2}\dots$ . The infinite word has no loops, and hence  $\omega_{\text{ex}}$  is an eSAW.

When we choose boundary conditions for a lattice model, conventionally this boundary is in real space, i.e. it applies to a piece of the lattice. In contrast, we consider eSAW to be SAW with periodic boundary conditions in what we could loosely describe as chain space. In chain space, SAW and eSAW are one-dimensional objects, regardless of the embedding dimension.

We are principally interested in the asymptotic behavior of the number of eSAW of  $n$  steps,  $e_n$ , and the square end-to-end distance  $er_n$  (other quantities of interest are defined in Sec. 2.5). In analogy with (1.3)–(1.5) we expect that:

$$e_n \sim A_e \mu_e^n n^{\gamma_e - 1} \left( 1 + \frac{a_1}{n} + \frac{a_2}{n^2} + \dots + \frac{b_0}{n^{\Delta_1}} + \dots \right) + \text{AF}, \quad (2.1)$$

$$er_n \sim A_e D_e \mu_e^n n^{2\nu_e + \gamma_e - 1} \left( 1 + \frac{f_1}{n} + \frac{f_2}{n^2} + \dots + \frac{g_0}{n^{\Delta_1}} + \dots \right) + \text{AF}, \quad (2.2)$$

$$e\rho_n \sim D_e n^{2\nu_e} \left( 1 + \frac{l_1}{n} + \frac{l_2}{n^2} + \dots + \frac{m_0}{n^{\Delta_1}} + \dots \right) + \text{AF}, \quad (2.3)$$

where  $e\rho_n \equiv er_n/e_n$ .

In Sections 2.1-2.6 we will specialize to discussing eSAW on  $\mathbb{Z}^d$ , and will discuss the minor differences arising for the honeycomb lattice in Sec. 2.7.

## 2.1 Proof that $\mu_e = \mu$ for eSAW on $\mathbb{Z}^d$

Every bridge of  $n$  steps is also an eSAW of  $n$  steps, since by construction bridges can be concatenated with themselves (indeed, any bridge can be concatenated with any other bridge and remain self-avoiding). It is also clear that every eSAW is in fact a SAW, and hence if  $b_n$  is the number of bridges of  $n$  steps,  $e_n$  is the number of eSAW of  $n$  steps, and  $c_n$  is the number of SAW of  $n$  steps, we must have

$$b_n \leq e_n \leq c_n. \quad (2.4)$$

Therefore we must have

$$\lim_{n \rightarrow \infty} b_n^{1/n} \leq \lim_{n \rightarrow \infty} e_n^{1/n} \leq \lim_{n \rightarrow \infty} c_n^{1/n}, \quad (2.5)$$

but it has been proved [14] that

$$\lim_{n \rightarrow \infty} b_n^{1/n} = \lim_{n \rightarrow \infty} c_n^{1/n} = \mu \quad (2.6)$$

Thus, we have

$$\mu_e \equiv \lim_{n \rightarrow \infty} e_n^{1/n} = \mu, \quad (2.7)$$

i.e. the connective constant for eSAW is precisely the same as that for self-avoiding walks.

There is strong evidence that  $b_n$  and  $c_n$  obey the scaling laws:

$$b_n \sim n^{b-1} \mu^n \quad (2.8)$$

$$c_n \sim n^{\gamma-1} \mu^n \quad (2.9)$$

where  $b < 1^1$ . This in turn implies that  $b \leq \gamma_e \leq \gamma$ ; we will argue in the following subsection that in fact  $\gamma_e = 1$ .

## 2.2 Argument that $\gamma_e = 1$

We will now give a number of heuristic arguments in support of our expectation that  $\gamma_e = 1$ . Our intent is to communicate the intuition we have as to *why*  $\gamma_e = 1$ .

<sup>1</sup>In fact for two-dimensional lattices numerical evidence and SLE arguments provide convincing evidence that  $b = 9/16$ . Private communication from A. J. Guttmann.

Direct renormalization group arguments regarding the partition function for linear polymer models such as SAW in two and three dimensions lead to  $\gamma > 1$  [15, 16, 17]. Heuristically, this is due to the fact that ends have more freedom than the interior of the chain, and the degree of freedom increases as the length of the chain increases. See Chapter XI.1.6 of [15] for a qualitative but more detailed argument, and [16] for theoretical arguments regarding polymer networks with an arbitrary number of ends. See [17] for a systematic renormalization group calculation for linear polymers in conformation space, which explicitly showed the leading order contribution which perturbs  $\gamma$  away from 1 is due to an end effect.

For clarity we reproduce part of the argument of [15] here. Suppose we can express the free energy  $F$  of a polymer chain in terms of length  $n$  and interaction strength  $u$ . Then, if we renormalize the chain by a scale factor  $g$  by integrating out the structure at small length scales, we would expect that we could express the free energy of the full chain in terms of the free energy of the renormalized chain as follows:

$$F(n, u) = \Delta F(n, u) + F(n/g, u_1). \quad (2.10)$$

We are interested in the behavior of  $F$  in the vicinity of the fixed point  $u^*$ , where  $u \approx u_1 \approx u^*$ . For SAW,  $\Delta F$  includes a contribution from interior chain segments, which have two neighbors, and an additional contribution from the ends, which only interact with one neighbor. It is the contribution of the ends that perturbs  $\gamma$  away from 1.

For SAW, the enhancement effect becomes negligible for dimensions  $d > 4$  where  $\gamma = 1$ , while there is a logarithmic correction to the number growth in dimension four. For models where the ends have less freedom than the interior of the chain, such as bridges and SAP, we would expect (and do indeed observe) that the growth exponent is strictly less than unity.

Now, the complete absence of any end-effects for eSAW should mean that  $\gamma$  is *precisely* equal to 1, as there is no physical mechanism to perturb the value of  $\gamma$ . For eSAW,  $\Delta F$  in (2.10) only includes contributions from interior chain segments, and hence  $\gamma_e = 1$ .

We may consider eSAW as an object extending to infinity (a rooted self-avoiding chain, in the notation of Sec. 2.5). When we directly renormalize a configuration, its global nature remains invariant as it is still extends to infinity, and only the local structure of the walk changes. The one large scale alteration is the size of the repeating unit, or alternatively the density of boundaries along the walk. For SAW, the sizes of the end-regions of the walks scale in a different way to the interior of the chain. That is, for SAW there is an internal length scale (distance from the ends) which must be taken into account when the system is renormalized, but for eSAW there is no such length scale to worry about.

The ability to derive a model with  $\gamma = 1$  via the imposition of periodic boundary conditions is thus seen as fundamentally due to the fact that linear polymers are one-dimensional objects, no matter the dimensionality of the space they are embedded in. We therefore believe it is unlikely that other lattice models can be adapted in the same way. Of course, this does not preclude the possibility that a new insight could lead to non-trivial two-dimensional and three-dimensional models with  $\gamma = 1$ .

We note in passing that the process by which  $\gamma$  may be altered from its standard value is somewhat subtle: theoretical arguments suggested that it should be possible to vary  $\gamma$  [18] by introducing orientation dependent interactions into the polymer model. In particular, it was predicted that  $\gamma$  would be different for SAW on the Manhattan lattice [19] than on other lattices due to the fact that SAW cannot be trapped on this lattice (effectively introducing an orientation dependent interaction). However, detailed numerical investigation [20] subsequently showed that  $\gamma$  was unchanged from its value for SAW on other two-dimensional lattices.

Another ‘endless’ walk model is of course the model of self-avoiding returns. The number of self-avoiding returns grows as  $n^{\alpha-2}\mu^n$ , and the hyperscaling relation  $d\nu = 2 - \alpha$  can be interpreted in the following way. SAW with free end-points have typical size  $n^\nu$ , and so the fraction which return to the origin should be  $O(n^{-d\nu})$ . Thus we should expect the number of SAR to be

$$\#(SAR) \sim n^a n^{-d\nu} \mu^n, \quad (2.11)$$

where  $n^{-d\nu}$  is the factor due to geometric restriction, and  $n^a$  is an enhancement factor which parallels the  $n^{\gamma_e-1}$  factor for eSAW. There is strong theoretical and numerical evidence in support of the hyperscaling relation, which implies that  $a = 0$ . Since there are no geometric restrictions for eSAW, we regard the validity of the hyperscaling relation for self-avoiding returns to provide support for our argument that  $\gamma_e = 1$ .

We readily acknowledge that our arguments for  $\gamma_e = 1$  fall far short of a proof, and will verify  $\gamma_e = 1$  to good precision via series analysis methods in Sec. 4.

### 2.3 Argument that $\nu_e = \nu$

eSAW are different from SAW in that they have no ends, and so in a small region of the chain near the end one may expect that, on average, eSAW and SAW are qualitatively different. However, the size of SAW and similar objects

is dominated by the region of the chain far from the end, and this is why SAW, SAP, bridges, and eSAW all have the same size exponent  $\nu$ .

More explicitly, following Caracciolo et al. [21], we define

$$\xi_n^2 = \frac{1}{2d} \rho_n, \quad (2.12)$$

$$\varrho = \frac{|\mathbf{r}|}{\xi_n}. \quad (2.13)$$

Then in the limit  $n \rightarrow \infty$ ,  $|\mathbf{r}| \rightarrow \infty$ ,  $\varrho$  fixed, we expect that the end-to-end distribution function for SAW is [22, 21]

$$P(\varrho) = \frac{1}{\xi_n^d} f(\varrho) (1 + O(n^{-\Delta_1})) \quad (2.14)$$

where for large  $\varrho$

$$f(\varrho) \approx f_\infty \varrho^\sigma \exp(-D\varrho^\delta), \quad (2.15)$$

with  $\sigma$  and  $\delta$  both positive. Now, eSAW are a subset of SAW, and so if we suppose that  $\nu_e > \nu$ , then (2.15) would imply that  $e_n$  could not grow asymptotically as  $e_n \sim n^a \mu^n$ . The most reasonable interpretation, based on the assumption that  $e_n \sim n^a \mu^n$  and  $e\rho_n \sim n^{2\nu_e}$ , is that  $\nu_e \leq \nu$ .

In addition, we expect that eSAW which return close to the origin are suppressed, i.e. polygon-like configurations are relatively rarer amongst eSAW than they are amongst SAW. The endless condition induces an effective repulsion between the end-points, and thus we would expect that  $\nu_e \geq \nu$ . Therefore we conclude that  $\nu_e = \nu$ .

As an aside, we expect that the end-point repulsion would result in a larger amplitude for the mean square end-to-end distance for eSAW than for SAW.

## 2.4 Analytic corrections to scaling

For SAP on two-dimensional lattices, there is strong numerical evidence that the *non-analytic* corrections to scaling fold into the analytic background term [23, 24, 8].

For eSAW, we expect that the *analytic* corrections to scaling will fold into the analytic background term, due to the fact that  $\gamma_e = 1$ . If we define the generating function for the number of eSAW as

$$C_e(x) = \sum_{n=1}^{\infty} e_n x^n, \quad (2.16)$$

then we expect that the asymptotic behavior of the  $e_n$  series is determined by the singularity or singularities of  $C_e(x)$  which are closest to the origin. Neglecting the sub-leading anti-ferromagnetic singularity (which may have zero amplitude for eSAW in any case; see Sec. 5.3), we expect that

$$C_e(x) = \mathcal{A}(x) + \mathcal{B}(x)(1 - x/x_c)^{-\gamma_e} (1 + c(1 - x/x_c)^{\Delta_1} + \dots), \quad (2.17)$$

where  $\mathcal{A}(x)$  and  $\mathcal{B}(x)$  are analytic functions. If we write

$$\mathcal{B}(x) = A_e + \beta_1(1 - x/x_c) + \beta_2(1 - x/x_c)^2 + \beta_3(1 - x/x_c)^3 + \dots, \quad (2.18)$$

then, under the assumption that  $\gamma_e = 1$ , all of the higher order terms with coefficients  $\beta_1, \beta_2, \beta_3, \dots$  will be absorbed into the analytic background term  $\mathcal{A}(x)$ !

Thus, in (2.1) we expect that  $a_1 = a_2 = \dots = 0$ . We will test this hypothesis, as there could conceivably be a confluent logarithmic correction which would result in non-zero coefficients  $a_i$ .

## 2.5 Irreducible eSAW and self-avoiding chains

The more natural definition of an endless SAW (to us), which we will call a self-avoiding chain (SAC), is related to eSAW in the same way that self-avoiding polygons are related to self-avoiding returns. SAC are equivalence classes of eSAW which correspond to the same ‘shape’, regardless of the root point, or the direction of traversal.

For an  $n$ -step eSAW on  $\mathbb{Z}^d$  there are  $n$  possible root points, and two directions of traversal, suggesting that the number of eSAW of  $n$  steps should be  $2n$  times the number of SAC. However, there is an additional complication for the eSAW / SAC correspondence which does not occur for self-avoiding returns / self-avoiding polygons: eSAW can have repeating sub-units which makes the infinite chain corresponding to a given eSAW non-unique. We illustrate this in Fig. 2.2, where it can be seen that the same infinite chain results for the two eSAW shown. We call those

eSAW with no repeating units *irreducible* eSAW. The number of eSAW,  $e_n$ , and the square end-to-end distance  $r_n$  can then be straightforwardly expressed in terms of the number irreducible eSAW,  $i_n$ , and the square end-to-end distance of irreducible eSAW,  $ir_n$ :

$$e_n = \sum_{j|n} i_j, \quad (2.19)$$

$$er_n = \sum_{j|n} \frac{n^2}{j^2} ir_j. \quad (2.20)$$

The inverse expressions can be obtained, if desired, via a Möbius transform involving the Möbius function  $\mu$ :

$$i_n = \sum_{j|n} \mu\left(\frac{n}{j}\right) e_j, \quad (2.21)$$

$$ir_n = \sum_{j|n} \mu\left(\frac{n}{j}\right) \frac{n^2}{j^2} er_j. \quad (2.22)$$

An alternative interpretation is that the word corresponding to an irreducible eSAW cannot be decomposed into identical, repeating sub-words.

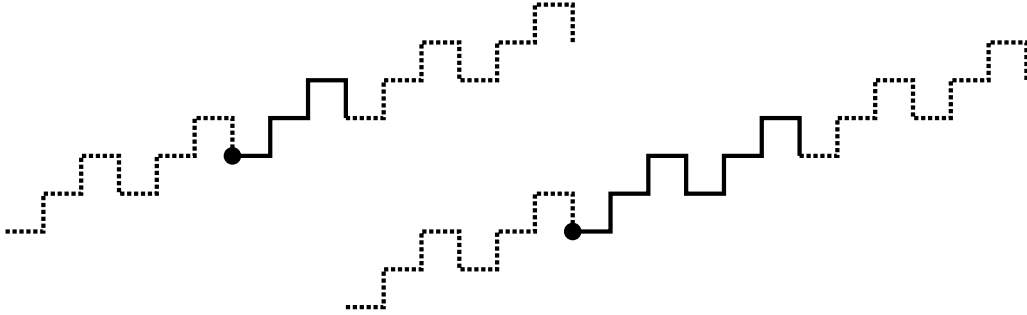


Figure 2.2: Examples of two eSAW which correspond to the same infinite chain. The eSAW on the left is irreducible.

Note that one does not need to worry about “irreducible” SAR configurations precisely because of the self-avoidance condition. If we were to consider *weakly* as opposed to *strictly* avoiding self-avoiding returns / polygons instead then the same complication would occur, as loops could then repeat.

Now for each irreducible eSAW of  $n$  steps there are  $n$  possible root points, as can be seen for our example eSAW in Fig. 2.3. In addition there are two possible orientations for the walk, and hence there  $2n$  irreducible eSAW for each self-avoiding chain. If we denote the number of SAC with an irreducible unit of  $n$  steps as  $d_n$ , then

$$i_n = 2nd_n. \quad (2.23)$$

In terms of words, converting from rooted to unrooted eSAW can be done by enforcing an ordering on the set of words corresponding to a given chain, and then choosing a single representative of this set. A natural way to do this is to use lexicographic ordering by placing an order on the steps themselves, e.g.  $1 < \bar{1} < 2 < \bar{2}$ . In Fig. 2.3 this results in the ordering  $12121\bar{2} < 121\bar{2}12 < 1\bar{2}1212 < 2121\bar{2}1 < 21\bar{2}121 < \bar{2}12121$ ; the eSAW in the top left of the figure,  $12121\bar{2}$ , would thence be chosen as the representative. Orientation independence on words can be enforced by defining words which are mapped to each other under the involution  $1 \leftrightarrow \bar{1}$  and  $2 \leftrightarrow \bar{2}$  to be equivalent.

In summary, endless walks may be reducible or irreducible, rooted or unrooted, and oriented or unoriented. Using this taxonomy, the objects we will study in this paper are shown in Table 1. We expect that the asymptotic behavior of the irreducible and reducible series will be *exactly* the same, i.e.  $i_n \sim e_n$  and  $ir_n \sim er_n$ . Since  $d_n = i_n/(2n)$ , the exponent for the growth in  $d_n$  is  $(\gamma_e - 2)$  instead of  $(\gamma_e - 1)$ , but otherwise the asymptotic growth for  $d_n$  is given in (2.1).

We show the self-avoiding chains with irreducible units of 1-4 steps in Fig. 2.4.

## 2.6 Properties of eSAW

We will now briefly mention some properties of eSAW which may not be immediately apparent.

Firstly, although all bridges are eSAW, the converse is not true. For example, the eSAW in Fig. 2.5 is not a bridge, and no choice of start and end points on the self-avoiding chain corresponding to the eSAW results in a bridge. A

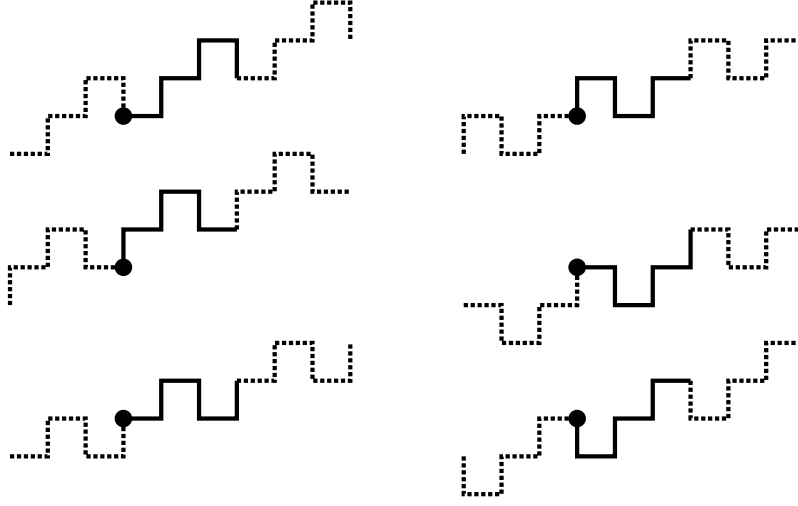


Figure 2.3: Irreducible eSAW which are equivalent up to the root point.

Object	Properties	Sequence
eSAW	reducible, rooted, oriented	$e_n$
	square end-to-end distance of eSAW	$er_n$
	mean square end-to-end distance of eSAW	$e\rho_n$
irreducible eSAW	irreducible, rooted, oriented	$i_n$
	square end-to-end distance	$ir_n$
	mean square end-to-end distance	$i\rho_n$
self-avoiding chains	irreducible, unrooted, unoriented	$d_n$

Table 1: Definitions of objects and their corresponding sequences.

necessary and sufficient condition for a SAC to allow for the choice of a bridge as the repeating unit, or equivalently for the word representation of an eSAW to have a cyclic permutation which is a bridge, is that there must exist a vertical line which cuts only a single bond of the SAC. The proof of this statement is obvious by inspection.

Going further, a natural generalization of bridges would be to allow for directions other than vertical for the cutting line. If all SAC were to admit at least one straight line which cuts only a single bond, then we would regard eSAW as a generalization of bridges. However, it is straightforward to derive eSAW for which any straight line must pass through at least two bonds of the SAC, for example by slightly perturbing the eSAW in Fig. 2.5.

Trapped self-avoiding walks are SAW which cannot be extended indefinitely from (at least) one of the ends and still remain self-avoiding (see e.g. [25]). By definition, no trapped self-avoiding walk is an eSAW. Conversely, every non-trapped self-avoiding walk is a sub-walk of an infinite number of eSAW, since the walk can always be extended far away from any problematic regions. Equivalently, all eSAW are Kesten patterns [26], and we expect that all patterns have positive density in sufficiently long eSAW. Examples of trapped and non-trapped SAW are shown in Fig. 2.6.

Unlike SAW, eSAW in dimensions  $d > 2$  allow for true knots to occur when we consider them as infinite chains. An example knotted eSAW is shown in Fig. 2.7; it corresponds to the word  $11\bar{2}\bar{3}\bar{3}\bar{2}\bar{2}\bar{1}333\bar{2}\bar{2}\bar{3}\bar{3}21$ , and is of length 17. This compares to the shortest knotted SAP on the simple cubic lattice, which has 24 steps [27, 28]. We do not know if 17 is the minimum length for an eSAW knot on the simple cubic lattice.

Finally we note that in two-dimensions all eSAW must have zero winding angle. The winding angle has featured in recent proofs of exact results for self-avoiding walks [7, 29].

## 2.7 eSAW on the honeycomb lattice

The set of direction vectors for the neighboring sites of the honeycomb lattice depends upon which of two bipartite sub-lattices one is currently on. This contrasts with the other lattices considered in this paper which possess full translation invariance. As a consequence, our definition of eSAW implies that on the honeycomb lattice eSAW may only have an even number of steps. An example of an eSAW for the honeycomb lattice is shown in Fig. 2.8. This

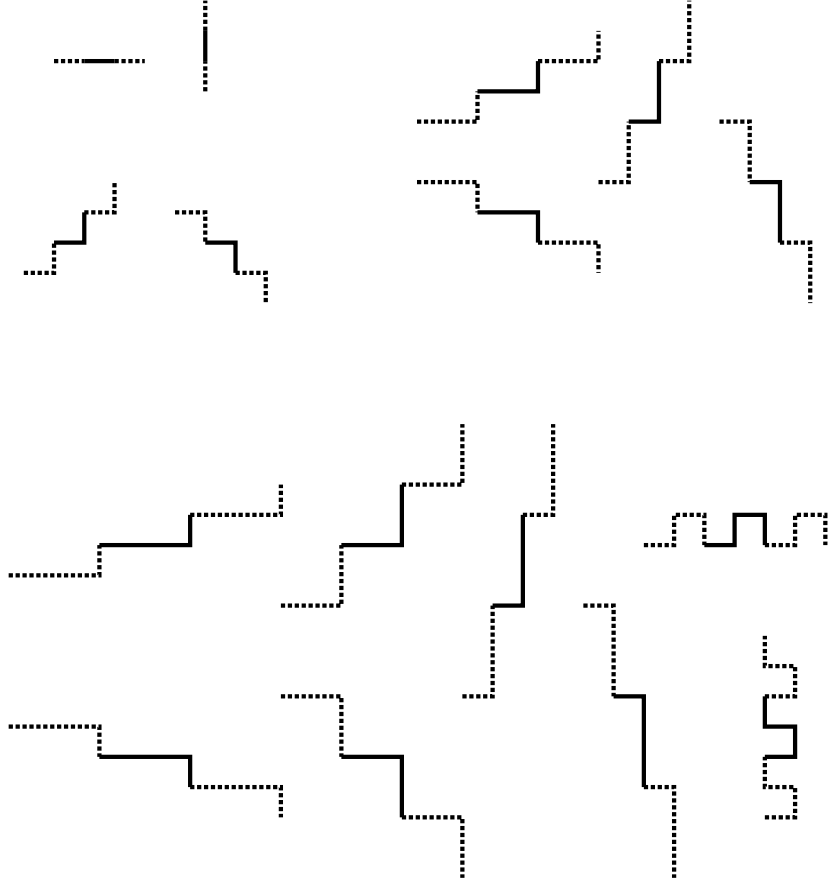


Figure 2.4: The self-avoiding chains with irreducible units of 1-4 steps on the square lattice. By inspection,  $d_1 = 2$ ,  $d_2 = 2$ ,  $d_3 = 4$ , and  $d_4 = 8$ , in agreement with the values in Table 2 of A.

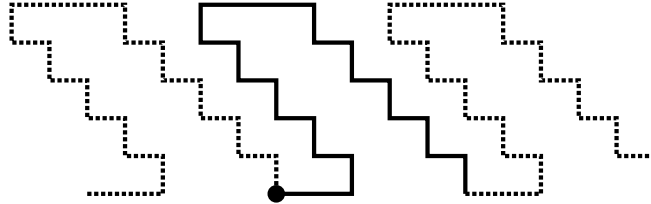


Figure 2.5: An eSAW for which no cyclic permutation is a bridge.

in turn means that a  $2n$  step self-avoiding chain on the honeycomb lattice has  $n$  possible root points, rather than  $2n$ . The relations between the different sequences must be modified accordingly:

$$e_{2n} = \sum_{j|n} i_{2j}, \quad (2.24)$$

$$er_{2n} = \sum_{j|n} \frac{n^2}{j^2} ir_{2j}, \quad (2.25)$$

$$i_{2n} = \sum_{j|n} \mu\left(\frac{n}{j}\right) e_{2j}, \quad (2.26)$$

$$ir_{2n} = \sum_{j|n} \mu\left(\frac{n}{j}\right) \frac{n^2}{j^2} er_{2j}, \quad (2.27)$$

$$i_{2n} = 2nd_{2n}, \quad (2.28)$$

where once again  $\mu$  is the Möbius function.



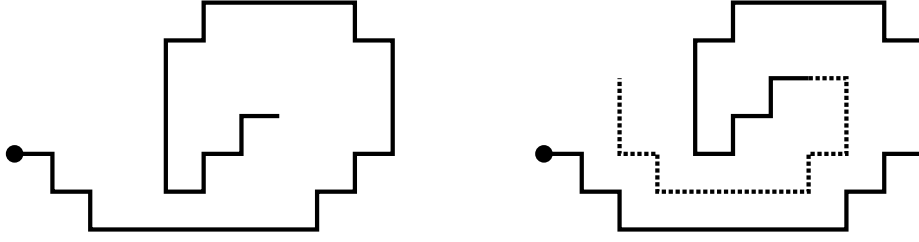


Figure 2.6: In solid lines, a trapped SAW on the left and a non-trapped SAW on the right (a possible continuation is shown as a dotted line). Neither of these are eSAW, but the non-trapped SAW may be a sub-walk of an eSAW.

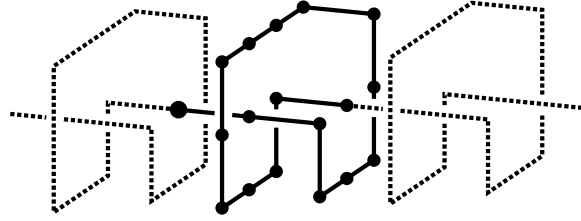


Figure 2.7: A knotted eSAW.

It is possible to broaden the definition of eSAW to allow for eSAW with an odd number of steps by altering the boundary conditions, e.g. by interchanging left turns and right turns at the concatenation point. However, this introduces some technical difficulties<sup>2</sup>, and in the absence of a pressing reason to do so we will not explore this option further here.

One key advantage for the analysis of eSAW on the honeycomb lattice is that the connective constant is known to be exactly  $\sqrt{2 + \sqrt{2}}$  [5, 7]. We will exploit this fact later in our analysis in Sec. 4.

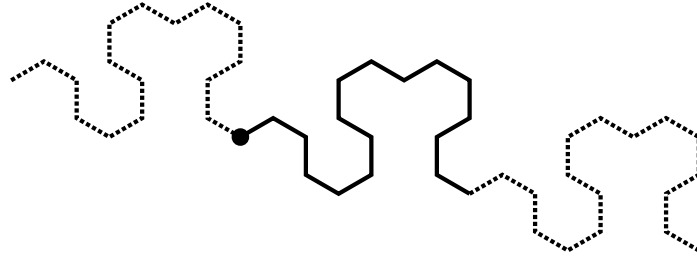


Figure 2.8: Example eSAW on the honeycomb lattice. Note that the repeating unit has an even number of steps; if one step were removed then the eSAW would no longer be able to remain on the honeycomb lattice.

The arguments for  $\nu_e$  and  $\gamma_e$  are not altered for the honeycomb lattice. However, the proof that  $\mu_e = \mu$  would need to be modified. We will not prove that  $\mu_e = \mu$  here, but are confident that this statement is indeed correct.

### 3 Enumeration method

We performed enumerations on the square, honeycomb, union jack, simple cubic, bcc, and fcc lattices using a basic backtracking algorithm. Backtracking works by explicitly generating all of the combinatorial objects of interest by recursively building up these objects from smaller objects.

We will not describe backtracking in detail, but note that it has been used to study SAW and related models for over 50 years (see section 7.3 of [30] for references). Here we focus on the differences between our algorithm for enumerating eSAW and the standard backtracking approach for enumerating SAW. More details on how to implement a backtracking algorithm for the enumeration of SAW are given in [9].

<sup>2</sup>E.g., in this context it seems more natural to use ‘mid edges’ as in [7] to define an eSAW with twisted boundary conditions, because a single edge does not carry any information about whether a left or right turn comes next.

The key difference between backtracking enumeration of eSAW and SAW, is that as an eSAW is built up step by step one has to check for self-intersections for the whole infinite chain. This is apparently quite a non-local effect, but it can in fact be converted to a local interaction provided the end-to-end vector is known.

Suppose we have end-to-end vector  $\mathbf{v}$ , then if we know that  $\mathbf{x}$  is a site on the walk then necessarily all sites  $\mathbf{y} = \mathbf{x} + j\mathbf{v}, j \in \mathbb{Z}$  must also be part of the endless walk. We should therefore test for self-intersections for an endless walk  $\omega$  by checking for self-intersections in reduced coordinates  $\omega(i)/\mathbf{v}$ .

Our algorithm generated all eSAW with a given end-to-end vector,  $\mathbf{v}$ , and used reduced coordinates to test for self-intersections. Starting at the origin, we incrementally grow our walk by considering all possible ways of adding an additional step which are compatible with the end-to-end vector. As the walk is extended we add  $\omega(i)$  to the list of visited sites, and we check to see if  $\omega(i)/\mathbf{v} = \omega(j)/\mathbf{v}$  for any  $j < i$ . If there is an intersection we know that this sub-walk can never be a valid eSAW, and so we truncate the backtracking tree.

The reduced coordinates of visited sites were stored in a hash table to ensure that intersection testing took  $O(1)$  CPU time. Optimal backtracking implementations take CPU time which is of exactly the same order as the number of objects being generated, and in this sense our implementation was optimal. It certainly would be possible to obtain a small constant factor improvement in performance through fine tuning the implementation.

We performed our enumerations on the following lattices in two dimensions: square, triangular, honeycomb, and union jack, and in three dimensions: simple cubic, body centered cubic (bcc) and face centered cubic (fcc). The two-dimensional lattices are shown in Fig. 3.1. The lattice we refer to as “union jack” is non-standard, as it allows for crossings, and may be properly described as a square lattice with additional bonds connecting next-to-nearest neighbors [31, 32].

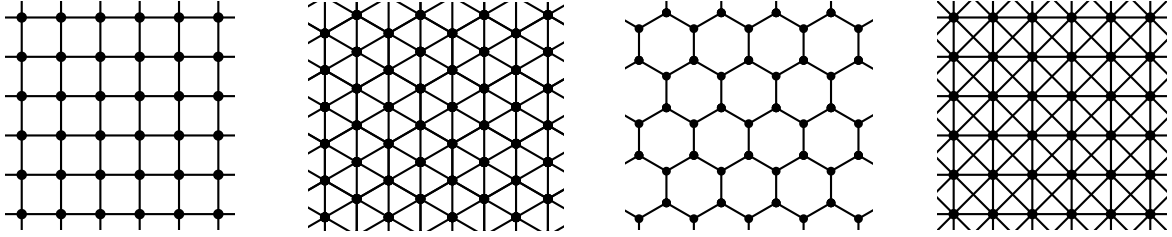


Figure 3.1: Two-dimensional lattices, from left to right: square, triangular, honeycomb, and union jack.

We enumerated  $e_n$  and  $er_n$  directly, and the fact that the resulting value for  $d_n$  must be an integer places quite a strong consistency condition on our enumerations. Another condition that our enumerations should satisfy comes from the observation that eSAW form equivalence classes under transformations of the underlying lattice. For the square lattice, eSAW which explore both available dimensions must form an equivalence class under the full symmetry group,  $O(2)$ , which means that  $e_n - 4$  must be divisible by 8. The corresponding condition for the simple cubic lattice is that  $e_n^{(\text{simple cubic})} - 3e_n^{(\text{square})} + 6$  must be divisible by 48, the number of elements of  $O(3)$ . We have confirmed that each of these conditions hold for our data.

Interestingly, SAC do not necessarily exhibit the full symmetry group of the underlying lattice. The symmetries under which SAC are invariant is determined purely by the end-to-end vector.

The combination of integer values for  $d_n$ , correct symmetry factors for  $e_n$ , and correct low order values gives us confidence that the enumerations reported in Tables 2–4 in A are correct. As an aside, we note that for  $n$  prime, the sequences must satisfy

$$e_{2n} = i_{2n} + i_2 = 2nd_{2n} + 2d_2 \quad \text{honeycomb lattice,} \quad (3.1)$$

$$e_n = i_n + i_1 = 2nd_n + 2d_1 \quad \text{all other lattices.} \quad (3.2)$$

We performed our enumerations on a SunFire X4600M2 with 2.3GHz AMD Opteron CPUs. For each lattice we divided the backtracking enumeration amongst 20 different processors. The total number of CPU hours required for the enumerations was: 12000 for the square lattice, 2100 for the triangular lattice, 2400 for the honeycomb lattice, 2000 for the union jack lattice, 5600 for the simple cubic lattice, 7000 for the bcc lattice, and 1300 for the fcc lattice.

Our enumeration data are collected in Tables 2–4 in A. Note that we only report  $r_n$  for the square and simple cubic lattices. A bug in our enumeration program for the other lattices meant that the data we collected suffered from rounding errors. These data would allow us to estimate the amplitude  $D_e$ , but since it is a non-universal quantity we regard  $D_e$  to be of relatively minor interest. We will present enumerations of  $r_n$  for other lattices in future papers.

Finally, note that we do not regard basic backtracking as best practice for performing the enumerations, rather as a sensible first step towards studying this new model. We briefly mention alternative enumeration approaches in the following subsection.

### 3.1 Alternative enumeration methods

More sophisticated enumeration algorithms hold promise for future progress, but implementing them for eSAW will require overcoming certain challenges due to the apparent non-locality of eSAW self-interactions. Our intuition is that this may present a significant technical challenge for the approaches mentioned below, but not an insurmountable obstacle.

The most straightforward approach to improving our enumerations would be to implement the two-step method [9]. This could certainly be used to extend the series in A by a few terms in each case for the same computational effort. We are not sure if the lace expansion technique described in the same paper could be useful for enumerations of eSAW.

The most powerful known method for three-dimensional walks is the length-doubling algorithm [33, 34]. It is not clear to us how this exciting new enumeration algorithm could be applied to eSAW.

We believe the most promising approach is the finite lattice method [35, 36], which has been applied to the problem of enumerating SAW [37] and SAP [38] on two-dimensional lattices. A recent improvement to the finite lattice method [38] raises the possibility that the method could also be usefully applied in three dimensions.

## 4 Analysis

Our goal in analyzing the series from Appendix A is to extract as much information as possible. In particular we wish to provide numerical support for our argument that  $\gamma_e = 1$  in Sec. 4.3 and  $\nu_e = \nu$  in Sec. 4.4. In Sec. 4.5 we provide evidence for the surprising fact that the amplitude  $A_e$  is universal, while confirming that there are no analytic corrections to scaling for the number growth.

For our analyses we use arguably the two most powerful, general purpose methods of series analysis available: the methods of direct fitting and differential approximants. We succinctly describe each of these methods below in Sections 4.1 and 4.2 respectively.

In our analyses we will ruthlessly exploit our prior knowledge of critical parameters, in particular the values of the connective constants of the various lattices. For two-dimensional lattices, the best estimates for  $\mu$  come from series derived from the finite lattice method. For the square lattice,  $\mu = 2.638\,158\,530\,35(2)$  [38], while for the triangular lattice  $\mu = 4.150\,797\,226(26)$  [39]. For the honeycomb lattice we have the exact result  $\mu = \sqrt{2 + \sqrt{2}} = 1.847\,759\,065\,022 \dots$  [5, 7]. For the union jack lattice there are no accurate prior estimates of the connective constant, and so in contrast to the other series we perform unbiased fits. From a recent Monte Carlo calculation, we know that  $\mu = 4.684\,039\,931(27)$  [40] for the simple cubic lattice. Using the length-doubling algorithm, Schram [41] has derived series for the bcc and fcc lattices to 28 and 24 steps respectively. A preliminary analysis of these data leads to  $\mu = 6.530\,521(6)$  (bcc) and  $\mu = 10.037\,067(7)$  (fcc).

The values above for the connective constants are in all cases sufficiently accurate that we can consider them to be “exact”, i.e. we do not have to measure the effect of the error in the estimates of  $\mu$  on our fits. This is not usually the case with biased fits. Our situation is special because this knowledge comes from other sources, and  $\mu$  is known to much higher precision than could possibly be obtained from our short eSAW series. We have tested this assumption for ourselves, but will not discuss this issue any further in the analysis below.

We found that eSAW series are in every case somewhat better behaved than the irreducible eSAW series. Generically, they are quite different to begin with but then the fits converge for larger  $n$ , since they are asymptotically identical. We attribute this to the fact that for small  $n$  the effect of repeating sub-walks for composite  $n$  values is quite high, whereas when  $n$  is large this effect becomes negligible. To reduce visual noise only the eSAW series are plotted.

We are mindful of the following observation due to Guttmann [42] with reference to extrapolations from series analysis: “error bounds are generally referred to as (subjective) confidence limits, and as such frequently measure the enthusiasm of the author rather than the quality of the data.”. Where we give an explicit confidence interval for our estimates we will try to moderate our enthusiasm. We will also present all of our fits in graphical form so that readers can make their own judgments.

### 4.1 Direct fitting

The method of direct fitting involves fitting the asymptotic form for the series with the series coefficients. This approach is especially useful for finding amplitudes.

The idea is to truncate (2.1)–(2.3) at some finite order, and then fit a subset of coefficients from the corresponding series to this truncation. Rather than going in to any great depth about the general method, we will instead explain exactly what fits are performed in the analysis below. The most detailed explanation is in Sec. 4.3.

See [42, 9, 43] for detailed explanations of the direct fitting approach.

## 4.2 Differential approximants

In the method of differential approximants, the unknown generating function is represented by the solution to an ordinary differential equation of the form:

$$\sum_{i=0}^K Q_i(z) \left( z \frac{d}{dz} \right)^i f(z) = P(z). \quad (4.1)$$

The functions  $P$  and  $Q_i$  are polynomials, of degrees  $L$  and  $N_i$ . We choose  $0 \leq L \leq 10$ ,  $N_K \geq 3$  (which guarantees at least three regular singularities), and take  $Q_K$  to have highest-order coefficient equal to 1. We choose  $K = 2$  for the two-dimensional lattices, and  $K = 1$  for the three-dimensional lattices as these series are generally shorter. The order of the polynomials was chosen so that  $|N_i - N_j| \leq 3$ . Given coefficients  $a_0, \dots, a_N$ , the polynomials  $P, Q_i$  are chosen so that the polynomial  $\sum_{n=0}^N a_n z^n$  solves the differential equation to within an error of order  $z^{N+1}$ . This choice is made by solving a system of linear equations in  $L + K + 1 + \sum_{i=0}^K N_i$  unknowns, determined from  $N + 1$  known coefficients.

Once the approximant for a given choice of  $L$ ,  $K$ , and  $N_i$  has been determined, one may then find the singularities of the differential equation by determining the zeroes of  $Q_K(z)$ . The exponent corresponding to each regular singularity is then determined from the indicial equation. For the singularity  $z_i$ , the corresponding exponent is:

$$\lambda_i = K - 1 - \frac{Q_{K-1}(z_i)}{z_i Q'(z_i)}. \quad (4.2)$$

The physically relevant singularity is the nearest singularity on the positive real axis. If we denote this singularity as  $z_c$ , then the connective constant  $\mu = 1/z_c$ . We denote approximants which have singularities near the physical singularity, or clearly incorrect singularities on or near the positive real axis, as “defective”. To estimate  $z_c$  and the corresponding critical exponent we determine the leading singularity for a large number of choices of  $L$  and  $N_i$ , and prune defective approximants away. We then plot these approximant estimates of the critical exponent against  $n$  (the power of the highest order series coefficient used) in order to extrapolate and obtain a final best estimate for the critical exponents  $\gamma_e$  and  $\nu_e$ .

If desired, it is straightforward to ensure that there is a singularity at a biased value of  $z_c$  by introducing an additional linear equation:

$$Q_K(z_c) = 0. \quad (4.3)$$

In this paper, we are able to utilize accurate estimates for  $\mu$  from longer SAW series, and so all of our differential approximant analyses are biased.

See Guttman [42] for far more information about differential approximants and series analysis, or Guttman and Jensen [43] for a recent overview.

## 4.3 $\gamma_e$

To determine  $\gamma_e$  for the square, honeycomb, and triangular lattices we take the logarithm of  $e_n/\mu^n$ , and note that the asymptotic form we derive from (2.1) is

$$\log(e_n/\mu^n) \sim (\gamma_e - 1) \log n + \log A_e + \left[ \frac{a_1}{n} + \frac{b_0}{n^{\Delta_1}} \right]. \quad (4.4)$$

We single out the leading order neglected terms by placing them in large square brackets. Note that we have substituted  $\mu$  for  $\mu_e$  due to the proof in Sec. 2.1. We then solve for  $\gamma_e$  and  $\log A_e$  by using terms from the sequence. For the triangular and honeycomb lattices we use consecutive terms, say  $e_{k-1}$  and  $e_k$  for the triangular lattice and  $e_{k-2}$  and  $e_k$  for the honeycomb lattice. For the square lattice we find that we obtain smoother fits by fitting alternate terms  $e_{k-2}$  and  $e_k$ . We label the resulting estimates for  $\gamma_e$  as  $\gamma_{e,k}$ , and plot these estimates in Fig. 4.1. Note that we choose to take the logarithm in the above equation simply as a matter of convenience, so that the equation to be solved for  $\gamma_e$  and  $\log A_e$  is linear.

Now, we expect that the error term in our  $\gamma_{e,n}$  fits is of the order of the first neglected term. The asymptotic behavior of two-dimensional SAW is well understood [8], thanks to a combination of series analysis of long series generated via the finite lattice method, and high powered Monte Carlo simulations. This leads us to believe that  $\Delta_1 = 3/2$  exactly. The argument of Sec. 2.4 suggests that  $a_1 = 0$ , and so we expect that plots of  $\gamma_{e,n}$  versus  $n^{-\Delta_1}$  should be linear, and this is confirmed for each lattice in Fig. 4.1. We confirmed that plots of  $\gamma_{e,n}$  versus  $1/n$  possess significant curvature, indicating that  $a_1$  must be close to zero in each case; we will estimate  $a_1$  in Sec. 4.5.

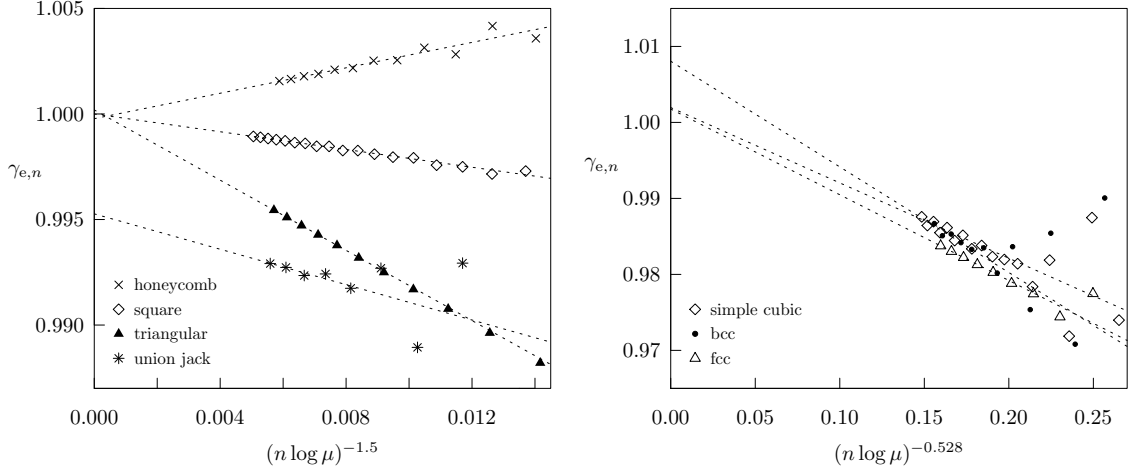


Figure 4.1: Direct fit estimates of  $\gamma_e$  for two- and three-dimensional lattices (left and right respectively).

We employ one additional trick in our plots of direct fit estimates. For a lattice with connective constant  $\mu$ , when we plot against a remainder of the form  $n^{-a}$  we normalize it as  $x = (n \log \mu)^{-a}$ . This ensures that for any given value of  $x$  the number of eSAW is approximately the same, independent of the lattice. Loosely speaking, we want the  $x$  coordinate to be correlated with the information content of the series.

We also obtain direct fits for  $\gamma_e$  from the union jack lattice, solving

$$\log e_n \sim n \log \mu + (\gamma_e - 1) \log n + \log A_e + \left[ \frac{a_1}{n} + \frac{b_0}{n^{\Delta_1}} \right] \quad (4.5)$$

for  $\log \mu$ ,  $\gamma_e$ , and  $\log A_e$  using coefficients  $e_{k-2}$ ,  $e_{k-1}$ , and  $e_k$ . These estimates are not as well behaved because we do not have the benefit of a prior high precision estimate for  $\mu$ .

Examining Fig. 4.1 it is clear that all of the estimates for  $\gamma_{e,n}$  are converging smoothly to 1, as predicted. As a visual guide we fit a straight line to the five highest order estimates for each lattice, and their y-intercepts are extremely close to 1, especially for our high precision data from the square, honeycomb and triangular lattices. From the figure,  $\gamma_e$  must be within the range 1.000(1). We could do better with the direct fits, but we will see that the differential approximant analysis below is more than adequate for the task of placing a tight bound on  $\gamma_e$ .

For the three-dimensional lattices, we once again fit the asymptotic form

$$\log(e_n/\mu^n) \sim (\gamma_e - 1) \log n + \log A_e + \left[ \frac{a_1}{n} + \frac{b_0}{n^{\Delta_1}} \right]. \quad (4.6)$$

For three-dimensional SAW, the asymptotic form is well understood theoretically, but the numerics are far more difficult. In [9] there is extensive discussion of the asymptotic form, while in [44] there is the most detailed and accurate numerical investigation of corrections to scaling that is currently available. For three-dimensional lattices we have  $\Delta_1 = 0.528(12)$  [44] as the dominant neglected term, but in other respects we proceed in the same manner as for the two-dimensional lattices. For the simple cubic and bcc lattices we fit  $e_{k-2}$  and  $e_k$ , while for the fcc lattice we fit  $e_{k-1}$  and  $e_k$ .

Our fits for  $\gamma_e$  are shown in Fig. 4.1. It is clear in each case that the estimates are smoothly converging to  $\gamma_e = 1$ . The fits as shown suggest that  $\gamma_e = 1.005(10)$ , which encompasses  $\gamma_e = 1$  as predicted. We do need to consider the effect of the known error in  $\Delta_1 = 0.528(12)$ , and so re-performed the analysis for  $\Delta_1 = 0.516$  and  $\Delta_1 = 0.54$ . In our case, because  $\Delta_1$  is known to high precision from another source, this does not materially change our estimate for  $\gamma_e$ .

As a technical aside, we find that for a number of lattices, particularly the square lattice, the simple cubic lattice, the bcc lattice, and to a lesser extent the honeycomb lattice, there is quite a high degree of oscillation with our direct fit estimates. We reduced the amplitude of the oscillations by fitting alternate terms, and on some occasions we also smoothed the fits by averaging consecutive estimates.

As mentioned in the description of the asymptotic forms (1.3)–(1.5), for SAW there is a contribution to the asymptotic form from the so-called anti-ferromagnetic singularity. In the analyses performed in this paper we avoid having to deal with this singularity directly by treating the series arising from odd and even terms separately. As explained in Sec. 5.3, there is no clear evidence as to whether the oscillations in the series are strictly odd-even, which would be a signal of the anti-ferromagnetic singularity on the negative real axis. The approximate alternation of some series is *not* conclusive, as it may be due to singularities near to but not on the negative real axis. Instead,

our choice to average consecutive terms and fit alternating terms is based purely on the observation that this makes the fits easier to extrapolate.

We now proceed to estimate  $\gamma_e$  for the various lattices via the differential approximant method described in Sec. 4.2. Our fits are reproduced in Figures 4.2, 4.3, and 4.4.

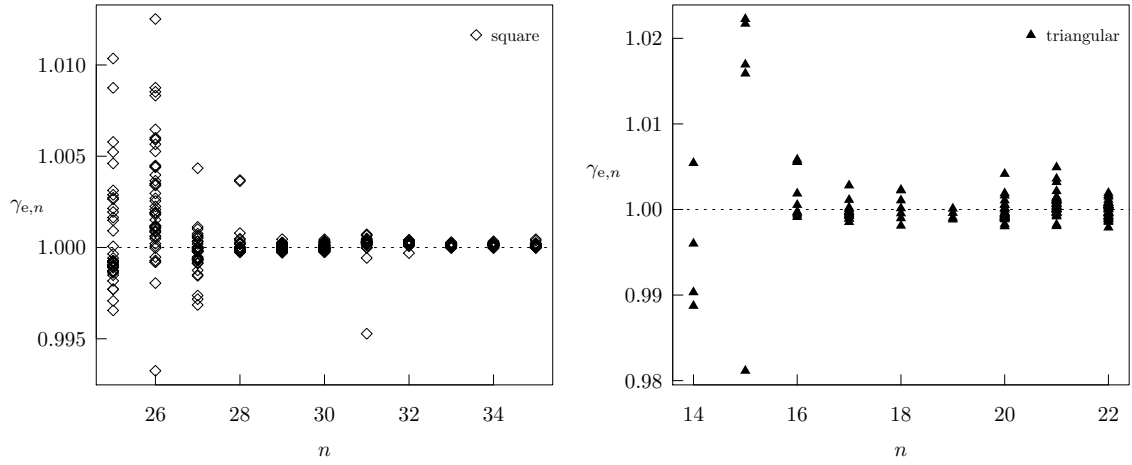


Figure 4.2: Differential approximant estimates of  $\gamma_e$  on the square (left) and triangular (right) lattices.

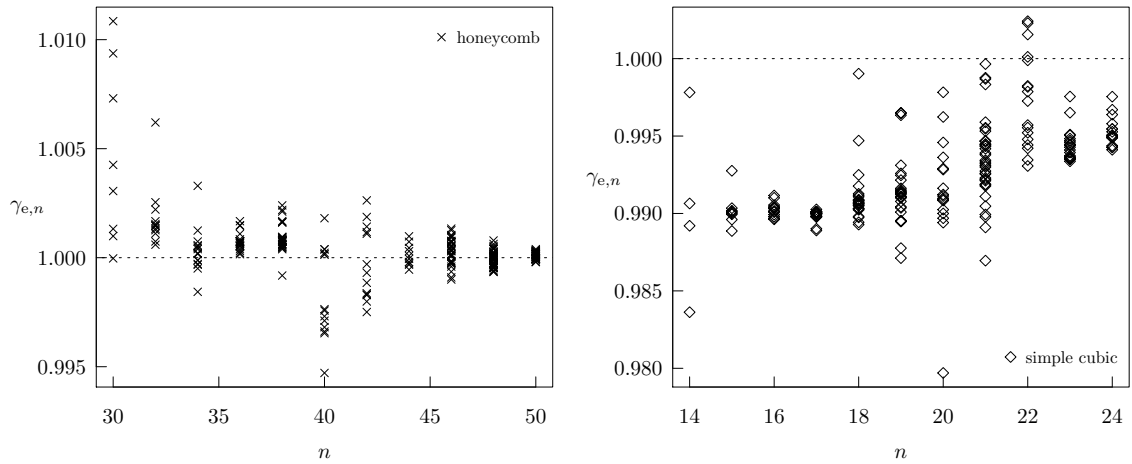


Figure 4.3: Differential approximant estimates of  $\gamma_e$  on the honeycomb (left) and simple cubic (right) lattices.

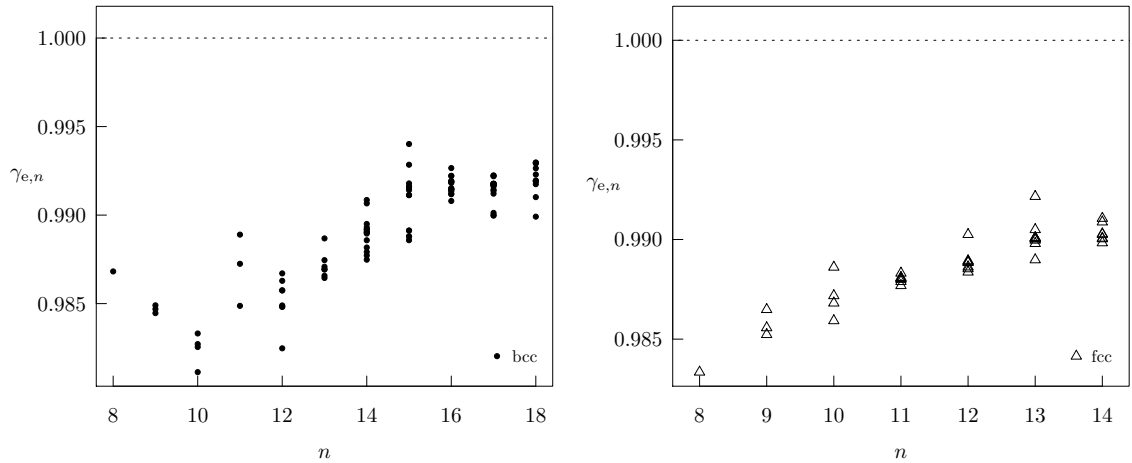


Figure 4.4: Differential approximant estimates of  $\gamma_e$  on the bcc (left) and fcc (right) lattices.

For the two-dimensional lattices, the differential approximants appeared to converge better for the square and honeycomb lattices. Nonetheless, combining information from all three suggests that  $\gamma_e = 1.000(1)$  in line with our direct fit estimate.

For the three-dimensional lattices the estimates are not as well converged, but this is to be expected because the series are shorter, and the leading correction to scaling is larger. Nonetheless, the trend in each case seems to be converging to one, and suggests that  $\gamma_e = 0.99(2)$ . We acknowledge that extrapolating such estimates is a fraught process, especially since there is clearly still systematic drift in the estimates. In addition, we already ‘know’ the answer, and this can easily introduce a subconscious bias. However, our interest here is less in deriving an estimate for  $\gamma_e$ , than in showing that  $\gamma_e = 1$  is the most plausible interpretation of the available evidence.

We consider the series analyses presented to be quite convincing in their support of our prediction that  $\gamma_e = 1$  for eSAW on two- and three-dimensional lattices. For the remainder of the analysis section we will *assume* that  $\gamma_e = 1$ , and use this information to bias our fits.

#### 4.4 $\nu_e$

For the purpose of estimating  $\nu_e$  we find that the  $er_n$  series is far more useful than the  $e\rho_n$  series. We only have reliable data for the square and simple cubic lattices, but we given that  $\nu_e$  is a universal quantity this is not a problem.

We assume that  $\gamma_e = 1$ , and substitute this into the asymptotic expression for  $er_n$ , and then perform direct fits on the following asymptotic form:

$$\log(er_n/\mu^n) \sim (2\nu_e + \gamma_e - 1) \log n + \log(A_e D_e) + \left[ \frac{f_1}{n} + \frac{g_0}{n^{\Delta_1}} \right], \quad (4.7)$$

$$\sim 2\nu_e \log n + \log(A_e D_e) + \left[ \frac{f_1}{n} + \frac{g_0}{n^{\Delta_1}} \right]. \quad (4.8)$$

For each of the lattices we fit alternating terms,  $e_{k-2}$  and  $e_k$ , to obtain estimates for  $\nu_{e,k}$  and the amplitude, and we plot the results in Fig. 4.5.

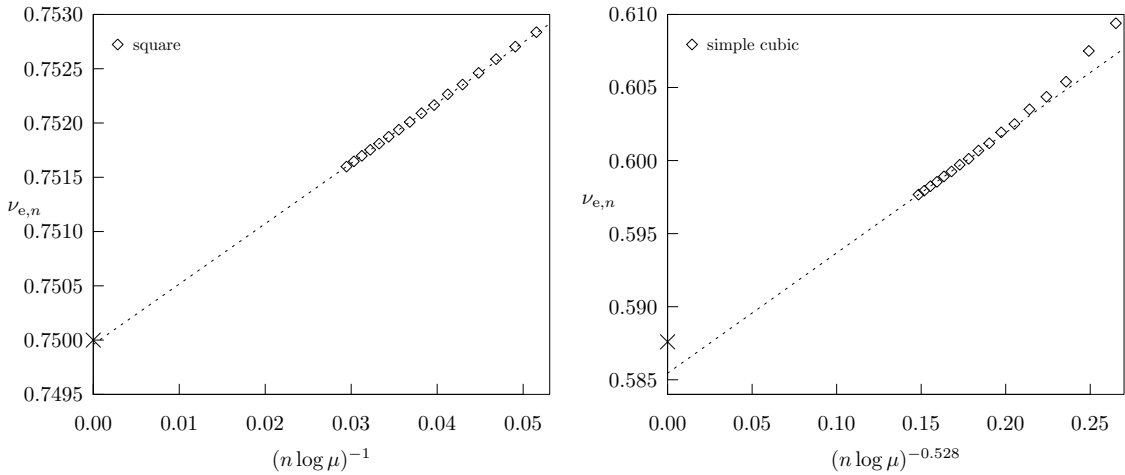


Figure 4.5: Direct fit estimates of  $\nu_e$  for the square (left) and simple cubic (right) lattices.

For the square lattice, it is very clear that the leading analytic correction to scaling has non-zero amplitude, as shown by the linear behavior of the fits in Fig. 4.5. The convergence to  $\nu_e = \nu = 3/4$  is extremely convincing; we conservatively interpret our results as suggesting  $\nu_e = 0.7500(1)$ .

For the simple cubic lattice, the convergence is not as good, but this is to be expected for such a short series with strong corrections to scaling. Our estimates in Fig. 4.5 suggest that  $\nu_e$  is in the vicinity of 0.586, while the best estimate for  $\nu$ ,  $\nu = 0.587\,597(7)$  [44], is shown on the plot.

The results from our differential approximant analyses are shown in Fig. 4.6. Technically, we are in fact plotting estimates of  $\nu_e + (\gamma_e - 1)/2$ , but we assume that  $\gamma_e = 1$  as stated previously.

For the square lattice the convergence of the differential approximants is very good, and  $\nu_e = 0.7500(1)$  is a conservative interpretation of the data.

For the simple cubic lattice, once again there is still a systematic drift occurring at  $n = 24$ , and the estimates for  $\nu_e$  are approximately clustered around 0.590-0.593. This is consistent with  $\nu_e = \nu$ , but not completely convincing.

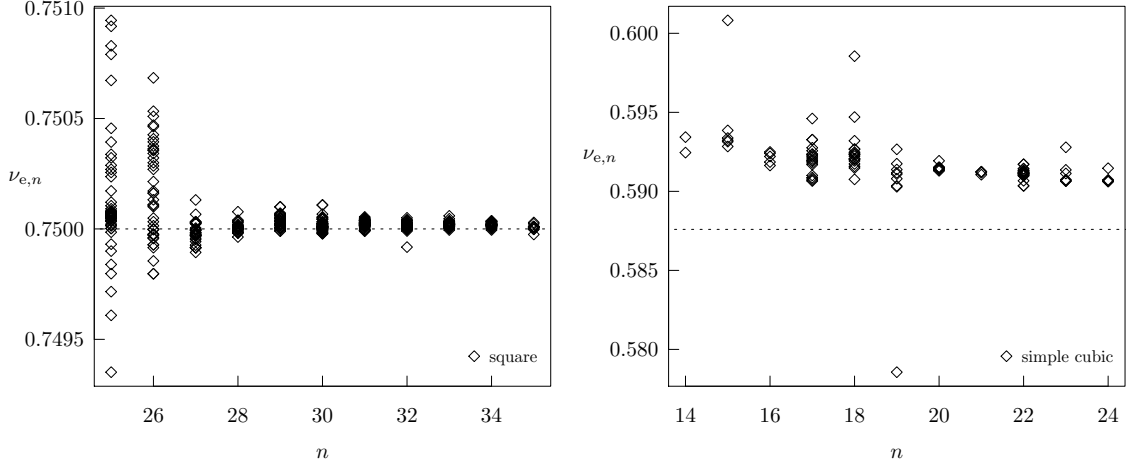


Figure 4.6: Differential approximant estimates of  $\nu_e$  on the square (left) and simple cubic (right) lattices.

We believe that the numerical evidence supporting  $\nu_e = \nu$  is unequivocal for the square lattice. For the simple cubic lattice we cannot be so definite due to the short series available, but we nonetheless strongly believe that  $\nu_e = \nu$  is the most plausible interpretation of the evidence for three-dimensional lattices also.

To obtain definitive evidence in support of  $\nu_e = \nu$  in three dimensions we will either need to significantly extend the series, or apply the pivot algorithm [44]. The pivot algorithm in the context of eSAW is discussed in Sec. 5.

#### 4.5 $A_e$

Assuming that  $\gamma_e = 1$ , the asymptotic form for  $e_n$  is given by:

$$e_n \sim A_e \mu^n n^{\gamma_e-1} \left( 1 + \frac{a_1}{n} + \frac{a_2}{n^2} + \cdots + \frac{b_0}{n^{\Delta_1}} + \frac{b_1}{n^{\Delta_2}} + \cdots \right), \quad (4.9)$$

$$\sim A_e \mu^n \left( 1 + \frac{a_1}{n} + \frac{a_2}{n^2} + \cdots + \frac{b_0}{n^{\Delta_1}} + \frac{b_1}{n^{\Delta_2}} + \cdots \right). \quad (4.10)$$

For the square, honeycomb, and triangular lattices we perform “direct fits” to

$$e_n/\mu^n \sim A_e + \left[ \frac{A_e a_1}{n} + \frac{A_e b_0}{n^{\Delta_1}} \right]. \quad (4.11)$$

In this case the fits are trivial: one merely has to calculate the ratio  $e_n/\mu^n$ . For the union jack lattice, we fit

$$\log e_n \sim n \log \mu + \log A_e + \left[ \frac{a_1}{n} + \frac{b_0}{n^{\Delta_1}} \right]. \quad (4.12)$$

We plot our estimates against  $1/n^{\Delta_1}$  in Fig. 4.7, noting that once again this gives clear linear trend which suggests that the analytic correction has zero amplitude.

We now observe a remarkable fact: our amplitude estimates appear to be converging towards the same constant. The coincidental convergence of the estimates from series from four different lattices seems highly unlikely, and thus we conclude that  $A_e$  is a universal quantity!

We test this conjecture further by *assuming* that  $a_0 = 0$ , and fitting

$$e_n/\mu^n \sim A_e + \frac{A_e b_0}{n^{\Delta_1}} + \left[ \frac{A_e a_2}{n^2} + \frac{A_e b_1}{n^{\Delta_2}} \right], \quad (4.13)$$

for the square, honeycomb, and triangular lattices only. We plot the resulting fits for  $A_e$  against the assumed form of the next-to-leading non-analytic correction, i.e.  $1/n^{5/2}$  [8]. Although we expect that  $a_2 = 0$  we do not rely upon this fact; essentially the same estimates are obtained for  $A_e$  from plots against  $1/n^2$ .

The resulting fits show a high degree of convergence. The scatter between the different lattices is consistent with there being non-trivial sub-leading corrections to scaling, which is not surprising for such short series.

We estimate that  $A_e = 1.57075(10)$  for two-dimensional eSAW. We note in passing that  $\pi/2 = 1.570796326794 \dots$  lies within the confidence interval of our estimate, although we have no theoretical basis for conjecturing that  $A_e = \pi/2$ .



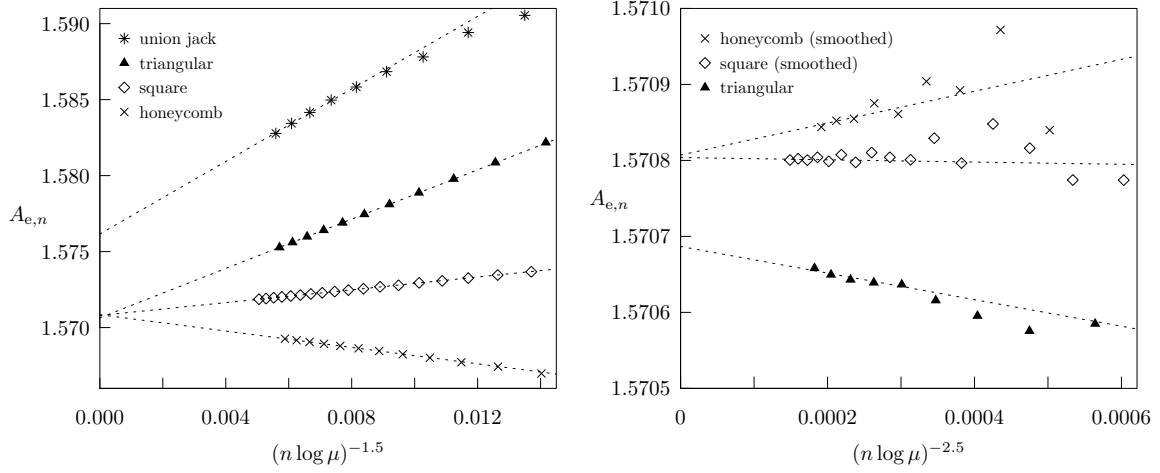


Figure 4.7: Direct fit estimates of  $A_e$  for two-dimensional lattices. On the left is the result of fitting asymptotic form with no correction to scaling, while on the right the leading correction to scaling is fitted.

For the simple cubic, bcc, and fcc lattices we perform direct fits to

$$e_n/\mu^n \sim A_e + \left[ \frac{A_e a_1}{n} + \frac{A_e b_0}{n^{\Delta_1}} \right], \quad (4.14)$$

and

$$e_n/\mu^n \sim A_e + \frac{A_e b_0}{n^{\Delta_1}} + \left[ \frac{A_e a_1}{n} + \frac{A_e b_1}{n^{\Delta_2}} + \frac{\text{const.}}{n^{2\Delta_1}} \right]. \quad (4.15)$$

For the simple cubic and bcc lattice we once again fit alternate values, while for the fcc lattice we fit consecutive values. We plot the resulting fits for  $A_e$  in Fig. 4.8. We plot the fits from (4.14) against the leading neglected term,

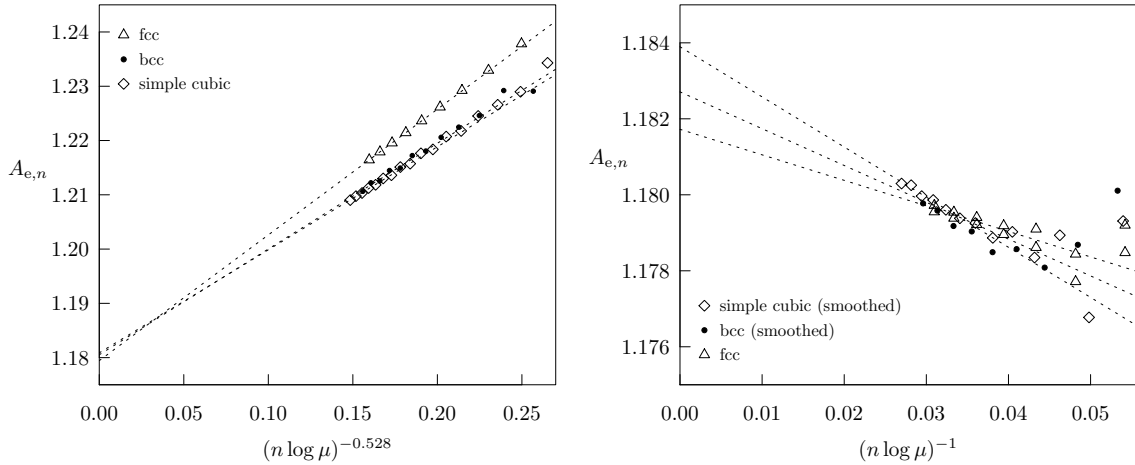


Figure 4.8: Direct fit estimates of  $A_e$  for three-dimensional lattices. On the left is the result of fitting asymptotic form with no correction to scaling, while on the right the leading correction to scaling is fitted.

$1/n^{\Delta_1}$ . For the fits from (4.15), even if the analytic correction to scaling in has zero amplitude there are still two competing non-analytic corrections with exponent in the vicinity of  $-1$ . Thus we plot fits from (4.15) against  $1/n$ .

Although we do not show these fits, we have tested the effect of using values of  $\Delta_1 = 0.528(12)$  within its error bar. In the fits from (4.15) this has the effect of extending the extrapolations to the vicinity of 1.180 and 1.185.

The estimates for  $A_e$  from all three lattices once again appear to be converging to a single value to good precision. This strongly suggests that  $A_e$  is a universal quantity for three-dimensional eSAW also. We estimate that  $A_e = 1.183(3)$

Finally, we will attempt to measure the amplitude of the leading analytic correction to scaling for two-dimensional

eSAW, which we expect to be identically zero. To do so, we fit

$$e_n/\mu^n \sim A_e + \frac{A_e a_1}{n} + \frac{A_e b_0}{n^{\Delta_1}} + \left[ \frac{A_e a_2}{n^2} + \frac{A_e b_1}{n^{\Delta_2}} \right], \quad (4.16)$$

for the square, honeycomb, and triangular lattices only. The inclusion of the  $\Delta_1$  non-analytic correction is necessary to be able to obtain sensible estimates for  $a_1$ . We plot the resulting estimates for  $a_1$  from all three lattices in Fig. 4.9. We plot the fits against  $1/n^{\Delta_2-1}$  since this is the relative size of the first unfitted term (assuming that  $a_2 = 0$ ).

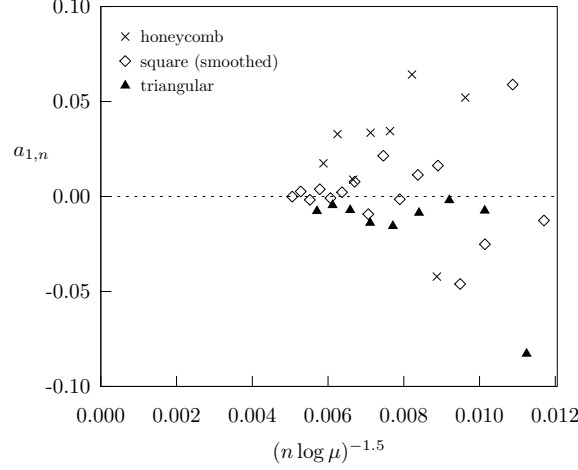


Figure 4.9: Direct fit estimates of the amplitude of the leading analytic correction to scaling,  $a_1$ , for the two-dimensional lattices.

We can see that for all three lattices the estimates for  $a_1$  are in the vicinity of zero, in agreement with our earlier observations based on the trends of our fits. The honeycomb lattice fits are still quite scattered, but the fits for the triangular and square lattices each suggest that  $a_1 = 0.00(2)$ . Although this is perhaps not as strong numerical evidence as that in favor of the universality of  $A_e$ , we nonetheless think that the evidence is convincing.

We do not attempt a similar analysis for the three-dimensional lattices, because there is no realistic possibility of obtaining meaningful fits for  $a_1$ . We discuss this further in Sec. 5.2.

## 5 Discussion

In the previous section, we confirmed that indeed  $\gamma_e = 1$  and  $\nu_e = \nu$  as we had predicted.

We now discuss our discovery that  $A_e$  appears to be universal in Sec. 5.1, the nature of corrections to scaling for  $e_n$  in Sec. 5.2, and the nature of the anti-ferromagnetic singularity for eSAW in Sec. 5.3. Then we mention some open questions for eSAW which will require further study in Sec. 5.4, before discussing some possible applications of eSAW in Sec. 5.5.

### 5.1 Universal amplitude

In Sec. 4.5 we presented strong numerical evidence that the amplitude for the number growth of eSAW is a universal quantity, with  $A_e = 1.57075(10)$  in two dimensions, and  $A_e = 1.183(3)$  in three dimensions. We had *not* anticipated this *a priori*, unlike the case for our argument that  $\gamma_e = 1$ . Indeed, the eSAW model was *constructed* with the goal of creating a model with  $\gamma_e = 1$ . We do have a heuristic *post hoc* argument to explain why the amplitude is universal, which we present below.

Once ends have been eliminated,  $\mu$  is simply a measure of local flexibility, and the polymer then only has one length scale, the Kuhn length. Once this length has been rescaled we must be left with a universal model, and since the length rescaling in  $A_e \mu^n$  occurs completely independently of the amplitude, this means that  $A_e$  must be a universal quantity.

We also observe that we now have an exact critical exponent relation,  $\gamma_e = 1$ , to which there should be a corresponding relation involving amplitudes.

It would be highly desirable to identify the critical amplitude with a standard quantity in the scaling theory of polymers.

We note in passing that this universal amplitude may serve as a signal of the  $\theta$  transition of interacting self-avoiding walks. We know that the amplitude of endless *simple* random walks is unity. For two-dimensional  $\theta$ -polymers we have  $\gamma = 8/7$  [45], and so we could expect that  $A_e$  for endless  $\theta$ -polymers would have a distinct value, i.e. it should lie between 1 and  $1.57 \dots$ . The upper critical dimension for the  $\theta$  transition is  $d = 3$ , and so for three-dimensional endless  $\theta$ -polymers it is likely that  $A_e = 1$ .

We will just make one further point. Amplitudes for lattice models, as opposed to amplitude ratios, are not typically universal quantities. For comparison, the amplitudes for SAW are  $A = 1.1449355(5)$  [46] for the honeycomb lattice, and  $A = 1.1770423(1)$  [37] for the square lattice. In contrast, the estimates for  $A_e$  from the square and honeycomb lattices agree to the fourth decimal digit.

## 5.2 Corrections to scaling

The analysis for eSAW on two-dimensional lattices in Sec. 4.5 supports our contention that there are no analytic corrections to scaling for the number growth, by confirming that the amplitude  $a_1$  from (2.1) is indistinguishable from zero for all lattices considered.

With longer enumerations from the finite lattice method it may be possible to estimate  $a_2$  or even  $a_3$ , which could strengthen this confirmation significantly. Monte Carlo simulations could also be used to improve the accuracy of the estimation of  $a_1$ .

We find clear evidence that the leading non-analytic correction to scaling for two-dimensional eSAW has exponent  $-3/2$ , which is the same as for two-dimensional SAW [8]. In particular, we do not see any evidence of the correction to scaling with exponent  $-11/16$ , predicted by CFT and observed for another recently invented SAW variant [12, 13].

For three-dimensional eSAW it is certainly possible that either the leading analytic correction to scaling has vanishing amplitude, or that there are no analytic corrections to scaling at all. However, it will be far more difficult to gather numerical evidence to resolve this question. This is because the leading non-analytic correction to scaling dominates the analytic correction, and in addition there are *two* non-analytic corrections which would compete with the leading analytic correction. The leading analytic correction has exponent  $-1$ , while the next-to-leading non-analytic corrections are  $-2\Delta_1 \approx -1.06$  and  $-\Delta_2$  which is believed to be close to  $-1$ . Consequently we consider the prospects of obtaining sufficiently strong numerical evidence to determine the amplitude of the leading analytic correction to be remote for three-dimensional eSAW.

Nonetheless, in the absence of a compelling argument for the existence of confluent logarithmic corrections, we consider it likely that there are no analytic corrections to scaling for three-dimensional eSAW.

## 5.3 Anti-ferromagnetic singularity

We have examined our series on the bipartite lattices - square, simple cubic, and bcc - for any evidence of the anti-ferromagnetic (AF) singularity (the honeycomb lattice is bipartite, but we are only considering one of the sub lattices). The AF singularity arises from polygon-like configurations: the odd-even effect is due to the fact that self-intersections can only occur between either two odd or two even sites of the walk.

The signature of the AF singularity for SAW is unambiguous for the same series lengths as we consider here for eSAW. From differential approximant analyses one can clearly detect the singularity on the negative real axis, at the correct location. From direct fitting, when we include an AF term in our fits we get clear signs of convergence to non-zero values for the fitted amplitudes. Finally, the inverses of the generating functions of interest provides a strong signal for the existence of the AF singularity [47].

For the case of eSAW, none of these analyses are conclusive!

For the bipartite lattice series, there is no clear signal from the DA analyses. On occasion, the differential approximants have singularities on the negative real axis, but the typical behavior is a strong signal of the critical point on the positive axis, and then other singularities scattered in the complex plane.

From the series themselves there are clearly oscillations, but the period in no case appears to be strictly two, and we have not been able to usefully apply the direct fitting approach.

Calculating the inverse of the generating functions, à la [47], leads to a strictly alternating series for SAW, but for eSAW on the square lattice there is no regular pattern at all, while for eSAW on the simple cubic and bcc lattices there is some hint that the series are settling down to something akin to alternation, but this is by no means definitive. Indeed, eSAW on the triangular lattice - which certainly does not have an AF singularity - displays a similar pattern to the simple cubic and bcc series.

In summary, the series analysis is inconclusive with respect to the existence of the AF singularity, and it may well be that the observed oscillations are determined by singularities in the complex plane.

We will now attempt to explain our intuition for whether there *should* be an AF singularity based on physical arguments. This is purely speculative, and in the absence of further numerical evidence should perhaps be given little weight.

For SAW, polygon-like configurations are the origin of the AF singularity: the dominant contributing configurations consist of large loops, and the odd-even effect arises from the interaction of the end-points.

For eSAW, polygon-like configurations are exponentially rare, as explained in Sec. 5.4. Large loops are possible, but the ends are then forced apart by the endless condition. Heuristically, for an eSAW of  $n$  steps,  $O(n)$  steps can be part of a large loop, but then  $O(n^\nu)$  steps are required for the end-points to escape from each other. We expect that this will result in the odd-even effect from the end-point interaction being exponentially suppressed or even eliminated completely, and hence no AF singularity will lie on the radius of convergence. It may be that our intuition is incorrect and that merely the amplitude of the AF singularity is suppressed, but our best guess is that the AF singularity is completely absent for eSAW.

In future, we will revisit this question with longer series in hand in an attempt to resolve this question definitively.

## 5.4 Open questions

One important topic for eSAW which we have not yet addressed is the behavior of eSAW with fixed end-points, and in particular the asymptotic behavior of  $e_n(x)$  as  $n$  approaches infinity with  $x$  fixed. For SAW, it is well known that

$$c_n(x) \sim B(x)\mu^n n^{2-\alpha}, \quad (5.1)$$

but the situation for eSAW is radically different. For eSAW in  $d$  dimensions, in the limit of large  $n$  it seems that the eSAW must become quasi  $(d-1)$  dimensional objects, with the eSAW effectively confined to a ‘slab’ with dimensions fixed by the end-to-end vector  $x$ . This slab could have quite a complicated structure, with the parallel surfaces allowed to have arbitrary shape provided that they are always separated by  $x$ . Thus it is not clear if the resulting eSAW would have growth constant of  $d-1$  dimensional SAW or a value that is intermediate between  $d-1$  and  $d$  dimensional SAW. The challenge is to understand and possibly predict the values of  $\kappa$ ,  $a$ , and  $B_e$  in

$$e_n(x) \sim B_e(x)\kappa^n n^a. \quad (5.2)$$

If eSAW in this limit are *exactly* like fixed end-point SAW in  $d-1$  dimensions, then we would expect that  $\kappa = \mu_{d-1}$  and  $a = -(d-1)\nu_{d-1}$ . This is a question that might be resolvable with a good theoretical argument, and it is also clearly desirable to study this question numerically.

Another important question is whether the pivot algorithm [48, 49] is ergodic for eSAW. One reason for the importance of this question is that recent improvements to the implementation of the pivot algorithm [50, 44, 51] have made it even more powerful. In addition, it is now clear that the pivot algorithm can be used for extremely accurate calculations of  $\mu$ ,  $\gamma$ , and  $\nu$  for SAW.

We expect that the pivot algorithm is indeed ergodic, since eSAW are very similar in nature to SAW, and in some sense they allow for less pathological behavior with respect to the pivot algorithm than SAW. This is true in the following sense: for SAW it is possible to form spiral structures with their ends which can only be unfurled extremely slowly with pivot moves. In contrast, for eSAW it is never possible for an end to become trapped, and thus it would seem that ‘most’ sites of a typical eSAW should be candidates for valid pivot moves. The key question is whether there are novel equivalence classes of eSAW which are invariant under pivot moves, which would result in non-ergodicity.

It may be difficult to prove that the pivot algorithm is indeed ergodic for eSAW. The difficulty lies in the fact that the non-local interactions change when a pivot is made, as the end-to-end vector typically changes after a successful move. Combining fixed end-point pivot moves [52, 53] with standard pivot moves might allow for a more straightforward proof, but this is a sub-optimal solution because fixed end-point moves are less efficient for the purpose of simulation. Application of the pivot algorithm to eSAW has not been the focus here, but it is a topic we intend to explore in the future.

Finally, much remains to be done regarding the application of theoretical techniques to eSAW. In particular, the renormalization group in conformation space [17] could be adapted to the study of eSAW, and should provide a strong theoretical argument that  $\gamma_e = 1$  in all dimensions.

## 5.5 Applications

Perhaps the application for which eSAW has the clearest advantage over the competing models of SAP and SAW is in the study of polymer knotting. Simulations for eSAW promise to be far more rapid than for SAP, provided the pivot algorithm with free end-point pivot moves can be proved to be ergodic (see Sec. 5.4).

At first glance, the eSAW series seem to hold less information than the corresponding SAW series of the same lengths, but it is quite possible that this is a short length effect, and that eSAW becomes superior to SAW at longer lengths. The absence of analytic corrections-to-scaling, and the possibility of deriving a theoretical prediction for the universal amplitude  $A_e$ , are significant advantages for eSAW over SAW. The large  $n$  limit can be probed via finite lattice method enumerations (perhaps approaching  $n = 80$  or so for the square lattice), and also via Monte Carlo simulation using the pivot algorithm (where  $n \gtrsim 10^8$ ). Thus we believe that eSAW hold considerable promise for allowing extremely accurate calculations for critical exponents and the connective constant for polymers in two and three dimensions.

Finally, we speculate that eSAW may be useful in the context of exact results on the honeycomb lattice [7, 29]. eSAW are a naturally defined special subset of SAW which have zero winding angle.

## 5.6 Generalizations

The concatenation idea of eSAW can be straightforwardly applied to other models of linear polymers, including interacting self-avoiding walks (ISAW) [54], the Domb-Joyce model of weakly interacting walks [55], and indeed continuum models such as bead-spring models. For these models, the interaction energy would need to be converted to an interaction energy per unit length, but other than that there are no significant complications. The self-avoiding trail model [56, 57, 58] and generalizations (e.g. [59]) could also be easily made ‘endless’.

One interesting consequence of the existence of a universal amplitude for the endless Domb-Joyce model, is that as the interaction parameter is varied, the (weighted) growth constant will vary while the amplitude will remain fixed. i.e. we would expect that for interaction strength  $J$ :

$$e_n(J) \sim A_e \mu(J)^n. \quad (5.3)$$

Of course this exactly what happens for  $\mu(J)$  and  $\gamma$  for the usual Domb-Joyce model.

It would be interesting to see if the eSAW idea could be extended to the continuum Edwards model [60].

As flagged in Sec. 2.7, it may be possible to allow for eSAW with an odd number of steps on the honeycomb lattice. More generally, the rule for concatenation of a walk with itself could be expanded to allow for symmetry operations such as reflections to be applied.

One weakness of the eSAW model is that there is no natural way to incrementally grow an eSAW. For a SAW, any sub-walk is also a SAW, but this is not true of eSAW. Interestingly, the set of eSAW for which any sub-walk is also an eSAW is precisely the set of directed walks. This can be seen straightforwardly by noting that: (a) If an eSAW has two steps in opposite directions, then the sub-walk which begins and ends with these steps is not an eSAW, and (b) Every directed walk is an eSAW. Perhaps there are other subsets of eSAW which may be of more interest.

It may be possible to study polymer networks using variations of eSAW, by concatenating together repeated copies of star or branched polymers. An example of a two-dimensional network created by such a recipe is shown in Fig. 5.1.

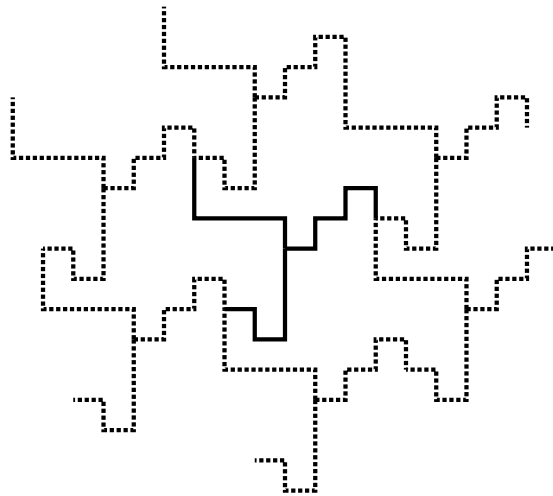


Figure 5.1: An example of a self-avoiding network created via concatenation of a star polymer on the square lattice.

## 6 Conclusion

We have introduced a new model of self-avoiding walks for which we have theoretical and numerical evidence that end-effects should be completely absent.

The enumeration results and analysis confirmed our expectations that  $\gamma = 1$  for eSAW, but more serious numerical work should be done to provide stronger confirmation. In future we will apply Monte Carlo techniques [49, 50, 44, 51] to accurately estimate critical exponents. It would be desirable to improve the rigor of our heuristic arguments that  $\gamma_e = 1$  and  $\nu_e = \nu$ .

We have made the surprising discovery that the eSAW model has a universal amplitude, and estimate that  $A_e = 1.57075(10)$  in two dimensions, and  $A_e = 1.183(3)$  in three dimensions. We have given one argument for this phenomenon, but it would be highly desirable to find other theoretical justifications. It remains to be seen if other models can be found which possess universal amplitudes. We also believe that there are no analytic corrections to scaling for the number growth of eSAW, and have supporting numerical evidence for two-dimensional eSAW.

The concatenation technique described in this paper can be straightforwardly applied to other models of polymers to create new ‘endless’ models. We are hopeful that the simple idea introduced here will open up a fruitful avenue of research.

## A Enumeration data

$n$	$e_n$	$er_n$	$i_n$	$d_n$
1	4	4	4	2
2	12	32	8	2
3	28	156	24	4
4	76	640	64	8
5	204	2380	200	20
6	540	8304	504	42
7	1404	27580	1400	100
8	3724	89216	3648	228
9	9748	280980	9720	540
10	25772	869360	25560	1278
11	67940	2649284	67936	3088
12	179068	7967808	178464	7436
13	472580	23722244	472576	18176
14	1245620	69977040	1244208	44436
15	3286308	204845220	3286080	109536
16	8666956	595628032	8663232	270726
17	22861604	1721605028	22861600	672400
18	60301764	4950241488	60291504	1674764
19	159063748	14167239268	159063744	4185888
20	419582396	40376066560	419556560	10488914
21	1106796012	114635882508	1106794584	26352252
22	2919664716	324361357936	2919596768	66354472
23	7701735292	914912704060	7701735288	167429028
24	20317148476	2573307218304	20316965760	423270120
25	53595401604	7218778025700	53595401400	1071908028
26	141385319932	20201661701936	141384847344	2718939372
27	372973583908	56408010198948	372973574160	6906918040
28	983913216292	157179257119360	983911970608	17569856618
29	2595592842460	437133635653148	2595592842456	44751600732
30	6847276871420	1213539966457200	6847273559040	114121225984
31	18063481834652	3363306014128316	18063481834648	291346481204
32	47652479932748	9306731807696384	47652471265792	744569863528
33	125710536151052	25715129922994380	125710536083088	1904705092168
34	331633319500804	70954363887188496	331633296639192	4876960244694
35	874875502020444	195525476447120540	874875502018840	12498221457412

Table 2: Enumeration data for the square lattice.

$n$	$e_n$	$er_n$	$i_n$	$d_n$
1	6	6	6	3
2	30	72	24	6
3	126	558	120	20
4	606	3744	576	72
5	2766	23070	2760	276
6	13134	135288	12984	1082
7	60990	764862	60984	4356
8	286014	4214784	285408	17838
9	1333926	22773798	1333800	74100
10	6235950	121158840	6233160	311658
11	29160390	636821526	29160384	1325472
12	136280046	3312601632	136266336	5677764
13	637801014	17087666310	637801008	24530808
14	2981709558	87499403544	2981648544	106487448
15	13958158806	445295758230	13958155920	465271864
16	65278026174	2253803314176	65277740160	2039929380
17	305608333062	11353558220742	305608333056	8988480384
18	1429710254742	56952225122616	1429708907808	39714136328
19	6693530115990	284620991825574	6693530115984	176145529368
20	31322452467006	1417625514526560	31322446230480	783061155762
21	146644481901582	7039475232292062	146644481840472	3491535281916
22	686366924272686	34860099689171064	686366895112272	15599247616188
23	3213444320539710	172198320473193822	3213444320539704	69857485229124
24	15042778398965358	848672945442198144	15042778262399904	313391213799998

Table 3: Enumeration data for the simple cubic lattice.

$n$	honeycomb ( $e_{2n}$ )	triangular	union jack	bcc	fcc
1	6	6	8	8	12
2	18	30	56	56	132
3	60	114	296	344	1284
4	210	486	1816	2312	12756
5	726	1986	10728	14648	126612
6	2448	8202	62648	96152	1265604
7	8448	33858	365464	622616	12652932
8	28818	140262	2130488	4066376	126616404
9	98556	580938	12424112	26456024	1267690812
10	336618	2407710	72464136	172470776	12697464132
11	1150320	9980394	422680024	1124590904	127218134748
12	3928944	41384106	2465699704	7328945336	1274923451364
13	13419204	171634482	14384367304	47829176312	12779117065740
14	45828192	711932538	83919450272	311758824440	128110554439020
15	156512220	2953394214	489611186736	2035191240584	
16	534463698	12253006566	2856635570680	13269735071816	
17	1825120584	50838740046	16667509269248	86634355605416	
18	6232259412	210946278126	97251708586688	565037351668904	
19	21281168202	875324356398			
20	72666555570	3632308990686			
21	248124503652	15073375131306			
22	847224827676	62553271396074			
23	2892836367066				
24	9877456541376				
25	33725891989626				

Table 4: Enumeration data for the honeycomb, triangular, union jack, bcc, and fcc lattices.

## Acknowledgments

I would like to thank Tony Guttmann for helpful discussions which led me to consider the anti-ferromagnetic singularity more deeply, and for comments on the paper. I would like to thank Mireille Bousquet-Mélou for comments which led me to consider the relationship between cyclic permutations of bridges and endless self-avoiding walks. Financial support from the ARC Centre of Excellence for Mathematics and Statistics of Complex Systems is gratefully acknowledged.

## References

- [1] Neal Madras and Gordon Slade. *The Self-Avoiding Walk*. Birkhäuser, Boston, 1993.
- [2] P. G. de Gennes. Exponents for the excluded volume problem as derived by the Wilson method. *Phys. Lett. A*, 38:339–340, 1972.
- [3] Takahashi Hara and Gordon Slade. Self-avoiding walk in five or more dimensions I. The critical behaviour. *Commun. Math. Phys.*, 147:101–136, 1992.
- [4] David Brydges and Gordon Slade. Renormalisation group analysis of weakly self-avoiding walk in dimensions four and higher. In *Proceedings of the International Congress of Mathematicians, Hyderabad*, 2010.
- [5] Bernard Nienhuis. Exact critical point and critical exponents of  $O(n)$  models in two dimensions. *Phys. Rev. Lett.*, 49:1062–1065, 1982.
- [6] Gregory F. Lawler, Oded Schramm, and Wendelin Werner. On the scaling limit of planar self-avoiding walk. In *Fractal Geometry and Applications: a Jubilee of Benoit Mandelbrot, Part 2. Proc. Sympos. Pure Math.*, volume 72, pages 339–364. Am. Math. Soc., Providence, 2004.
- [7] Hugo Duminil-Copin and Stanislav Smirnov. The connective constant of the honeycomb lattice equals  $\sqrt{2} + \sqrt{2}$ . *Ann. Math.*, 175:1653–1665, 2012.
- [8] Sergio Caracciolo, Anthony J. Guttmann, Iwan Jensen, Andrea Pelissetto, Andrew N. Rogers, and Alan D. Sokal. Correction-to-scaling exponents for two-dimensional self-avoiding walks. *J. Stat. Phys.*, 120:1037–1100, 2005.
- [9] N. Clisby, R. Liang, and G. Slade. Self-avoiding walk enumeration via the lace expansion. *J. Phys. A: Math. Theor.*, 40:10973–11017, 2007.
- [10] Timothy M. Garoni, Anthony J. Guttmann, Iwan Jensen, and John C. Dethridge. Prudent walks and polygons. *J. Phys. A: Math. Theor.*, 42:095205, 2009.
- [11] Mireille Bousquet-Mélou. Families of prudent self-avoiding walks. *J. Combin. Theory Ser. A*, 117:313–344, 2010.
- [12] Marco Gherardi. *Conformal Walks in Two Dimensions*. PhD thesis, University of Milan, 2009.
- [13] Marco Gherardi. Exact sampling of self-avoiding paths via discrete Schramm-Loewner evolution. *J. Stat. Phys.*, 140:1115–1129, 2010.
- [14] J. M. Hammersley. Percolation processes. *Math. Proc. Cambridge Phil. Soc.*, 53:642–645, 1957.
- [15] P. G. de Gennes. *Scaling Concepts in Polymer Physics*. Cornell University Press, 1979.
- [16] Bertrand Duplantier. Statistical mechanics of polymer networks of any topology. *J. Stat. Phys.*, 54:581–680, 1989.
- [17] Y. Oono and Karl F. Freed. Conformation space renormalization of polymers. I. Single chain equilibrium properties using Wilson-type renormalization. *J. Chem. Phys.*, 75:993–1008, 1981.
- [18] John Cardy. Continuously varying exponents for oriented self-avoiding walks. *Nucl. Phys. B*, 419:411–423, 1994.
- [19] D. Bennett-Wood, J. L. Cardy, I. G. Enting, A. J. Guttmann, and A.L. Owczarek. On the non-universality of a critical exponent for self-avoiding walks. *Nucl. Phys. B*, 528:533–552, 1998.
- [20] Sergio Caracciolo, Maria Serena Causo, Peter Grassberger, and Andrea Pelissetto. Determination of the exponent  $\gamma$  for SAWs on the two-dimensional Manhattan lattice. *J. Phys. A: Math. Gen.*, 32:2931–2948, 1999.
- [21] Sergio Caracciolo, Maria Serena Causo, and Andrea Pelissetto. End-to-end distribution function for dilute polymers. *J. Chem. Phys.*, 112:7693–7710, 2000.
- [22] Michael E. Fisher. Shape of a self-avoiding walk or polymer chain. *J. Chem. Phys.*, 44:616–622, 1966.
- [23] A. R. Conway and A. J. Guttmann. Square lattice self-avoiding walks and corrections to scaling. *Phys. Rev. Lett.*, 77:5284–5287, 1996.



- [24] Iwan Jensen and Anthony J. Guttmann. Self-avoiding polygons on the square lattice. *J. Phys. A: Math. Gen.*, 32:4867–4876, 1999.
- [25] Yao-ban Chan and Andrew Rechnitzer. A Monte Carlo study of non-trapped self-avoiding walks. *J. Phys. A: Math. Theor.*, 45:405004, 2012.
- [26] Harry Kesten. On the number of self-avoiding walks. *J. Math. Phys.*, 4:960–969, 1963.
- [27] Yuanan Diao. Minimal knotted polygons on the cubic lattice. *J. Knot Theory Ramif.*, 02:413–425, 1993.
- [28] Kyungpyo Hong, Sungjong No, and Seungsang Oh. Upper bounds on the minimum length of cubic lattice knots. *J. Phys. A: Math. Theor.*, 46:125001 (7 pp), 2013.
- [29] Nicholas R. Beaton, Mireille Bousquet-Mélou, Jan de Gier, Hugo Duminil-Copin, and Anthony J. Guttmann. The critical fugacity for surface adsorption of self-avoiding walks on the honeycomb lattice is  $1 + \sqrt{2}$ , 2012.
- [30] Barry D. Hughes. *Random Walks and Random Environments: Volume 1: Random Walks*. Random Walks and Random Environments. Oxford University Press, 1995.
- [31] J. Oitmaa. Self-avoiding walks with nearest- and next-nearest-neighbour steps. *J. Phys. A: Math. Gen.*, 13:L243–L246, 1980.
- [32] K. S. S. Narayanan and K. De’Bell. Self-avoiding walks including next-nearest-neighbor steps. *Phys. Rev. E*, 51:2644–2646, 1995.
- [33] R. D. Schram, G. T. Barkema, and R. H. Bisseling. Exact enumeration of self-avoiding walks. *J. Stat. Mech.*, 2011:P06019, 2011.
- [34] Raoul D. Schram, Gerard T. Barkema, and Rob H. Bisseling. SAWdoubler: A program for counting self-avoiding walks. *Comput. Phys. Commun.*, 184:891–898, 2013.
- [35] T. de Neef and I. G. Enting. Series expansions from the finite lattice method. *J. Phys. A: Math. Gen.*, 10:801–805, 1977.
- [36] I. G. Enting. Generating functions for enumerating self-avoiding rings on the square lattice. *J. Phys. A: Math. Gen.*, 13:3713–3722, 1980.
- [37] Iwan Jensen. Enumeration of self-avoiding walks on the square lattice. *J. Phys. A: Math. Gen.*, 37:5503–5524, 2004.
- [38] Nathan Clisby and Iwan Jensen. A new transfer-matrix algorithm for exact enumerations: self-avoiding polygons on the square lattice. *J. Phys. A: Math. Theor.*, 45:115202, 2012.
- [39] Iwan Jensen. Self-avoiding walks and polygons on the triangular lattice. *J. Stat. Mech.*, 2004:P10008, 2004.
- [40] Nathan Clisby. Calculation of the connective constant for self-avoiding walks via the pivot algorithm. *arXiv:1302.2106*, 2013.
- [41] Raoul Schram. Exact enumeration of self-avoiding walks. Master’s thesis, University of Utrecht, 2011.
- [42] A. J. Guttmann. On the critical behaviour of self-avoiding walks: II. *J. Phys. A: Math. Gen.*, 22:2807–2813, 1989.
- [43] Anthony J. Guttmann and Iwan Jensen. Series analysis. In Anthony J. Guttman, editor, *Polygons, Polyominoes and Polycubes*, volume 775 of *Lecture Notes in Physics*, pages 181–204. Springer Netherlands, 2009.
- [44] N. Clisby. Accurate estimate of the critical exponent  $\nu$  for self-avoiding walks via a fast implementation of the pivot algorithm. *Phys. Rev. Lett.*, 104:055702, 2010.
- [45] Bertrand Duplantier and Hubert Saleur. Exact tricritical exponents for polymers at the  $\Theta$  point in two dimensions. *Phys. Rev. Lett.*, 59:539–542, 1987.
- [46] Iwan Jensen. Honeycomb lattice polygons and walks as a test of series analysis techniques. *J. Phys.: Conf. Ser.*, 42:163–178, 2006.
- [47] Nathan Clisby and Gordon Slade. Polygons and the lace expansion. In Anthony J. Guttman, editor, *Polygons, Polyominoes and Polycubes*, volume 775 of *Lecture Notes in Physics*, pages 117–142. Springer Netherlands, 2009.

- [48] Moti Lal. ‘Monte Carlo’ computer simulation of chain molecules. I. *Mol. Phys.*, 17:57–64, 1969.
- [49] Neal Madras and Alan D. Sokal. The pivot algorithm: A highly efficient Monte Carlo method for the self-avoiding walk. *J. Stat. Phys.*, 50:109–186, 1988.
- [50] Tom Kennedy. A faster implementation of the pivot algorithm for self-avoiding walks. *J. Stat. Phys.*, 106:407–429, 2002.
- [51] N. Clisby. Efficient implementation of the pivot algorithm for self-avoiding walks. *J. Stat. Phys.*, 140:349–392, 2010.
- [52] N. Madras, A. Orłitsky, and L. A. Shepp. Monte Carlo generation of self-avoiding walks with fixed endpoints and fixed length. *J. Stat. Phys.*, 58:159–183, 1990.
- [53] E. J. Janse van Rensburg, S. G. Whittington, and N. Madras. The pivot algorithm and polygons: results on the FCC lattice. *J. Phys. A: Math. Gen.*, 23:1589–1612, 1990.
- [54] W. J. C. Orr. Statistical treatment of polymer solutions at infinite dilution. *Trans. Faraday Soc.*, 43:12–27, 1947.
- [55] C. Domb and G. S. Joyce. Cluster expansion for a polymer chain. *Journal of Physics C: Solid State Physics*, 5:956, 1972.
- [56] A. Malakis. Self-avoiding walks on oriented square lattices. *J. Phys. A: Math. Gen.*, 8:1885–1898, 1975.
- [57] A. Malakis. The trail problem on the square lattice. *J. Phys. A: Math. Gen.*, 9:1283–1291, 1976.
- [58] A. J. Guttmann. Lattice trails. I. Exact results. *J. Phys. A: Math. Gen.*, 18:567–573, 1985.
- [59] Andrea Bedini, Aleksander L. Owczarek, and Thomas Prellberg. Anomalous critical behavior in the polymer collapse transition of three-dimensional lattice trails. *Phys. Rev. E*, 86:011123 (10pp), 2012.
- [60] S. F. Edwards. The statistical mechanics of polymers with excluded volume. *Proc. Phys. Soc.*, 85:613–624, 1965.